Physics – Uspekhi **45** (7) 687 – 718 (2002)

REVIEWS OF TOPICAL PROBLEMS PACS numbers: 42.65.Dr, 42.65.Ky, 42.65.Re, 42.65.Wi

Ultrashort light pulses in hollow waveguides

A M Zheltikov

DOI: 10.1070/PU2002v045n07ABEH001086

Contents

Abstract. Ultrafast-optics applications of nonlinear-optical processes in gas-filled hollow fibers are briefly reviewed. The main physical processes behind the use of hollow fibers for efficient generation of unprecedentedly short light pulses, enhanced short-wavelength generation, and improvement of the sensitivity of nonlinear-optical gas-phase analysis are considered. These processes include self- and cross-phase modulation, coherent four-wave mixing, high-order harmonic generation, and stimulated Raman scattering. The methods to generate extremely short pulses, including few-cycle field waveforms, and to control such pulses are discussed.

A M Zheltikov Physics Department and International Laser Center,
M V Lomonosov Moscow State University,
Vorob'evy Gory, 119899 Moscow, Russian Federation
Tel. (7-095) 939 51 74. Fax (7-095) 939 31 13
E-mail: zheltikov@top.phys.msu.su

Received 23 August 2001, revised 29 October 2001
Uspekhi Fizicheskikh Nauk **172** (7) 743 – 776 (2002)
Translated by A M Zheltikov; edited by M V Magnitskaya

1. Introduction

Modern laser physics has approached the femtosecond borderline, and a breakthrough to the domain of attosecond pulses may be expected in the near future. Sub-10-fs light pulses have already become a routine tool of laser experiments [1 – 4] employed for high-temporal-resolution spectroscopy [5, 6] and generation of radiation within a broad spectral range, including the water window [7].

Sub-5-fs light pulses produced by different methods in recent years [8 – 10] are a unique tool for studying a broad class of physical, chemical, and biological processes, allowing an unprecedentedly high temporal resolution corresponding to one or two optical cycles to be achieved. The synthesis of pulses with a duration shorter than 4 fs through the generation of multiple Stokes and anti-Stokes sidebands in a Raman-active gas [11] and the experimental demonstration of the possibility of generating 250-as pulses (1 as $= 10^{-18}$ s) by phase-locking high-order optical harmonics [12] are among the most impressive recent achievements.

Many prominent results in nonlinear and ultrafast optics in the past few years have resulted from the use of gas-filled hollow-core dielectric waveguides. In particular, self-phase modulation (SPM) of laser pulses in such waveguides allowed the authors of Refs [8, 9] to produce light pulses as short as 4.5 fs. Hollow fibers play an important role in the synthesis of ultrashort pulses through multiple stimulated Raman scattering [11, 13 – 16].

Since the optical breakdown threshold for a gas filling the fiber is typically much higher than breakdown thresholds for conventional optical fibers, hollow fibers permit sufficiently powerful light pulses as short as a few cycles of optical field to be produced. The authors of Refs [8, 9], in particular, have employed hollow fibers to generate light pulses with durations corresponding to several cycles of optical field and energies up to several tens of microjoules. The method of laser-pulse compression proposed and implemented in Refs [8, 9] is currently widely used in femtosecond laser systems [3].

Thus, the guided-wave optics of ultrashort light pulses, which is closely related, as mentioned above, to gas-filled hollow fibers, is a new rapidly growing and exciting area of physics. Advances in this field offer new approaches to the generation of attosecond pulses, stimulating the development of attosecond science [4, 12, 17, 18], giving a new impetus to optical metrological applications of ultrashort pulses [19 – 21] and investigation of ultrafast processes in matter [22], and suggesting new approaches in the coherent control of quantum systems in physics, chemistry, and biology [23 – 28].

The considerable progress achieved in this area of research in recent years, making it possible to produce light pulses of extremely short durations and allowing the parameters of ultrashort pulses to be controlled in an efficient way, necessitates a systematic review of the most significant theoretical and experimental results in this field. Such an analysis is the main goal of this paper.

This review is organized in the following way. Section 2 briefly overviews applications of gas-filled hollow-fibers in nonlinear optics. A historical perspective is given on the main results obtained in nonlinear and ultrafast optics resulting from the use of hollow fibers.

Section 3 is devoted to the basic physical aspects of frequency conversion and formation of extremely short pulses in gas-filled hollow fibers. We will discuss the main physical processes involved in the formation and propagation of ultrashort light pulses in hollow fibers that provide specific knobs to control parameters of ultrashort pulses by means of nonlinear optics. The general physical principles of ultrashort-pulse synthesis from phase-locked equidistant spectral components resulting from high-order harmonic generation or multiple stimulated Raman scattering will be also considered. In Section 4, we will analyze self-phase modulation of a short laser pulse in a lossy gas-filled fiber.

Section 5 is devoted to the physical processes behind the possibility of producing ultrashort pulses with controlled parameters. Equations for third-harmonic generation (THG) in a hollow fiber including self- and cross-phase modulation (XPM) processes will be analyzed. The results of experimental studies devoted to third-harmonic and difference-frequency generation (DFG) in gas-filled hollow fibers are discussed in Section 6. These experimental data demonstrate the possibility of using hollow fibers for improving the sensitivity of nonlinear-optical methods of gas-phase analysis. Effects related to higher order waveguide modes will be discussed. In Section 7, we consider high-order harmonic generation in gas-filled hollow fibers. It will be shown that, due to the self-phase modulation of the pump pulse in a hollow fiber filled with a weakly ionizing gas, the phase mismatch may vary within the pump pulse, lowering the efficiency of harmonic generation and decreasing its sensitivity to the gas pressure. Section 8 then demonstrates that the mismatch between the group velocities of the pump pulse and the probe pulse may limit the minimum duration of ultrashort pulses synthesized from multiple Stokes and anti-Stokes sidebands produced in a Raman-active medium pre-excited with a short laser pulse. The pump and probe pulses can be group-velocity-matched in a gas-filled hollow fiber with an appropriate choice of the gas pressure, the inner fiber diameter, as well as waveguide modes of the pump and probe beams. Such an approach allows the number of Stokes and anti-Stokes sidebands generated in a laser-pre-excited Raman-active medium to be considerably increased, thus opening the possibility to noticeably reduce the duration of light pulses synthesized with the use of this technique. The idea of applying coherent-control methods to improve the efficiency of multiple Raman sideband generation is discussed.

In Section 9, we consider hollow waveguides with a structured periodic cladding, which allow the optical losses characteristic of hollow-waveguide modes to be substantially reduced. In Section 10, we will demonstrate that a combination of a diffraction grating and a mirror gives a compact optical element integrating a hollow waveguide and a photonic band-gap (PBG) structure, which offers new solutions to the problems of nonlinear and ultrafast optics. We will investigate transmission spectra of hollow planar photonic band-gap waveguides and provide a qualitative analysis of these waveguides using the coupled-mode theory. The physical factors enhancing nonlinear-optical processes in such hollow waveguides will be also discussed. The main results of our review will be briefly summarized in the Conclusion (Section 11).

2. Hollow fibers in the nonlinear optics of ultrashort pulses

The rapid technological and conceptual progress in femtosecond laser physics, including the development of different types of multilayer and chirped dielectric mirrors, has resulted in the creation of all-solid-state sufficiently compact laser systems capable of generating sub-10-fs light pulses [1 – 4]. Still, nonlinear-optical processes in gas media are one of the main directions in the ultrafast optics of high-power laser pulses, opening exciting avenues toward the attosecond range of pulse durations.

Nonlinear-optical phenomena occurring in gas media in the field of high-power short laser pulses have been extensively investigated for a long period of time (e.g., see classical monographs [29, 30]). Impressive progress has been achieved in high-order harmonic generation [31 – 37] and the production of coherent short-wavelength radiation (with a wavelength less than 2.4 nm [7]).

The predominant concept of nonlinear-optical experiments in rare-gas jets has involved until recently focused laser beams, ensuring sufficiently high power density of laser radiation. Limitations on the efficiency of harmonic generation with such an approach are associated with the short interaction lengths characteristic of this beam geometry.

A way to increase the length of nonlinear-optical interaction in a gas medium has been proposed by Miles et al. [38] back in 1977, when the possibility of a substantial (by three orders of magnitude) increase in the efficiency of nonlinear-optical interaction in a hollow dielectric fiber was demonstrated for a four-wave mixing process of coherent anti-Stokes Raman scattering. These experiments, in fact, opened a nonlinear-optical chapter in the history of hollow fibers.

Important theoretical aspects of four-wave mixing in gas-filled hollow fibers have been studied by Arkhipkin et al. [39]. The authors of Refs [8, 9] have shown that the use of a hollow optical fiber permits efficient spectral broadening of an ultrashort laser pulse due to self-phase modulation. In particular, it was demonstrated that 20-fs laser pulses propagating through a hollow fiber filled with a rare gas experience SPM-induced spectral broadening that is sufficient for subsequent pulse compression down to 4.5 fs.

Due to the possibility of using high-power laser pulses and large propagation lengths, the hollow-fiber technique also offers much promise for optical frequency conversion through coherent wave mixing and harmonic generation. Durfee et al. [40] have demonstrated that the use of hollow fibers provides an opportunity to achieve a high efficiency of optical frequency conversion in third-harmonic generation (up to 0.2%) and parametric four-wave mixing (up to 13%).

The authors of Ref. [40] also demonstrated that the phase mismatch related to waveguide dispersion in hollow optical fibers can compensate for the phase mismatch due to gas dispersion. The efficiency of nonlinear-optical interactions can be substantially improved under these conditions, opening the way to increase the energy of high-order harmonics and to control parameters of harmonics by varying the parameters of pump radiation [41, 42].

Subsequent intense investigations of nonlinear-optical wave-mixing processes in hollow fibers [43 – 47] have demonstrated that, due to the compensation of phase mismatch in these fibers, the efficiency of frequency conversion in high-order (up to the 45th order) harmonic generation can be increased by a factor of 100 – 1000 as compared with the efficiencies of frequency conversion attainable in experiments with gas jets [31 – 35]. Hollow fibers can also be used, as shown by experiments [47, 48], to improve the sensitivity and to expand the capabilities of gas-phase analysis based on coherent four-wave-mixing spectroscopy.

Theoretical analysis of Ref. [49] has revealed the possibilities of using sequential high-order harmonic generation in hollow fibers to increase the energy of harmonic radiation as compared to the case of direct harmonic generation. A gas-filled hollow fiber can be employed under these conditions as an efficient multifrequency source of coherent short-wavelength radiation.

Hollow fibers permit the pump and the signal generated through a frequency-nondegenerate nonlinear-optical process to be phase-matched. With a careful choice of the parameters of a hollow fiber, the gas pressure, and excitation of appropriate waveguide modes, the phase mismatch related to the gas dispersion can be compensated for by the waveguide component of the phase mismatch [40 – 42]. When these conditions are satisfied, the energy of the nonlinear signal can be considerably increased by using longer hollow fibers.

Parameters of short pulses of short-wavelength radiation generated through nonlinear-optical interactions in gas-filled hollow fibers can be controlled due to cross-phase modulation [41, 42]. This idea was implemented by Durfee et al. [50], who employed cross-phase modulation in parametric four-wave mixing in a gas-filled hollow fiber to achieve a high efficiency of frequency up-conversion with simultaneous pulse compression. Using 35-fs pulses of Ti:sapphire-laser radiation as a pump, Durfee et al. [50] demonstrated efficient generation of 8-fs pulses of 270-nm radiation upon the compensation of the XPM-induced chirp.

Thus, nonlinear-optical interactions of short pulses in hollow fibers suggest new ways of creating sources of ultrashort pulses in the UV range. Such sources would be useful for many practical applications, including high-temporal-resolution spectroscopy of atomic and molecular systems, investigation of ultrafast processes in solids, as well as medical and biological applications. In the following section, we will discuss in greater detail the basic physical processes allowing gas-filled hollow fibers to be used for achieving high efficiencies of frequency conversion and generating ultrashort light pulses with controlled parameters.

3. General physical aspects of the formation of ultrashort light pulses in hollow fibers

This section will be devoted to the analysis of general physical aspects of frequency conversion and ultrashort-pulse generation in gas-filled hollow fibers. We will briefly consider the basic physical processes contributing to the formation and propagation of ultrashort light pulses in hollow fibers and allowing different regimes of nonlinear-optical control of ultrashort pulses to be implemented. We will also discuss the basic physical principles of the synthesis of ultrashort pulses from phase-locked equidistant spectral components arising as a result of high-order harmonic generation or multiple stimulated Raman scattering.

3.1 The basic physical processes

The basic physical processes behind the formation and propagation of ultrashort light pulses with controlled parameters in hollow fibers include effects related to gas dispersion and dispersion of waveguide modes, self- and cross-phase modulation processes, sum- and difference-frequency generation due to multiwave mixing, high-order harmonic generation, stimulated Raman scattering, as well as processes related to the ionization of the gas filling the fiber.

In the regime of strong spectral broadening, modulation instabilities and shock-wave formation should also be taken into consideration. These effects distort the spectrum and the waveform of a short light pulse propagating through a fiber. However, in the first-order approximation, such effects can often be ignored. Each of the above-mentioned processes is examined in a more detailed way below.

3.1.1 Dispersion effects. Dispersion effects play the key role in the formation of ultrashort pulses. Generally, the dispersion frequency dependence of the refractive index of the gas filling the fiber leads to the distortion and spreading of light pulses. Dispersion effects also limit the efficiency of nonlinear-optical interactions, as they give rise to phase and group-velocity mismatches of light pulses.

Dispersion effects can be qualitatively understood in terms of the expansion of the wave number k as a power series in the frequency around the central frequency of the pulse ω_0 (obviously, such an approach may encounter difficulties in the case of light pulses as short as several field

cycles):

$$k(\omega) = k_0 + \frac{1}{u}(\omega - \omega_0) + \frac{1}{2}\, k_2(\omega - \omega_0)^2 + \ldots , \qquad (1)$$

where $k_0 = k(\omega_0)$, $u = (\partial\omega/\partial k)\big|_{\omega_0}$ is the group velocity of the pulse, and $k_2 = (\partial^2 k/\partial\omega^2)\big|_{\omega_0}$ is the group-velocity dispersion. The first term in expansion (1) describes effects related to the frequency dependence of the phase velocity of radiation in a medium, including phase mismatches in nonlinear-optical interactions. The second term in Eqn (1) results in group-delay effects in linear and nonlinear-optical processes. The third term is responsible for group-velocity dispersion, which is especially important for ultrashort light pulses.

This term describes the spreading and compression of short pulses. For media where we can restrict our analysis to the terms up to the second order in the expansion of dispersion relation (1), the complex amplitude of the pulse at the output of the medium $E(t)$ is related to the complex amplitude of the input pulse $E_0(t)$ by the following expression [51]:

$$E(t) = \frac{\exp(-\mathrm{i}k_0 z)}{(2\pi\mathrm{i}k_2 z)^{1/2}} \exp\frac{\mathrm{i}(t - z/u)^2}{2k_2 z} \times \int_{-\infty}^{\infty} E_0(t) \exp\left(\frac{\mathrm{i}\xi^2}{2k_2 z} - \frac{\mathrm{i}\eta\xi}{k_2 z}\right) \mathrm{d}\xi\,. \qquad (2)$$

Higher order dispersion effects distort the waveforms of light pulses, which often becomes a serious limiting factor in short-pulse formation and in ultrafast optics in general.

One of the main advantages of hollow fibers, which is extensively employed for the formation of ultrashort pulses and the enhancement of nonlinear-optical interactions of such pulses, is associated with the possibility of using the dispersion of guided modes to compensate for the gas dispersion [40–43]. The relation between the material and waveguide dispersion components can be tuned within a rather broad range by varying the inner radius of a hollow fiber and changing the gas pressure. This circumstance can be employed to achieve high efficiencies of frequency conversion and ultrashort-pulse formation (see Sections 6 and 7).

3.1.2 Self-phase modulation. Self-phase modulation is a phenomenon that results from the dependence of the refractive index of a medium (the gas filling the fiber in the case under consideration) on the intensity of a light pulse. In the case of light fields of moderate intensities, the refractive index of a medium can be written as

$$n = n_0 + n_2 I(t)\,, \qquad (3)$$

where n_0 is the refractive index of the medium in the absence of a light field, $n_2 = (2\pi/n_0)^2 \chi^{(3)}(\omega;\omega,\omega,-\omega)$ is the nonlinear refractive index [$\chi^{(3)}(\omega;\omega,\omega,-\omega)$ is the third-order nonlinear-optical susceptibility of the medium], and $I(t)$ is the intensity of laser radiation. Then, the nonlinear (intensity-dependent) phase shift of a pulse at a distance L is given by [29, 51]

$$\Phi(t) = \frac{\omega}{c}\, n_2 I(t) L\,. \qquad (4)$$

Due to the time dependence of radiation intensity within the light pulse, the nonlinear phase shift is also time-dependent, giving rise to a generally time-dependent frequency deviation:

$$\Delta\omega(t) = \frac{\omega}{c}\, n_2 L\, \frac{\partial I}{\partial t}\,. \qquad (5)$$

The resulting spectral broadening of the pulse can be estimated in the following way:

$$\Delta\omega = \frac{\omega}{c}\, n_2 L\, \frac{I_0}{\tau}\,, \qquad (6)$$

where I_0 is the peak intensity of the light pulse and τ is the pulse duration.

Thus, self-phase modulation results in the spectral broadening of a light pulse propagating through a hollow fiber. This effect allows compression of light pulses through the compensation of the phase shift acquired by the pulse in a hollow fiber. Compensation of a linear chirp, corresponding to a linear time dependence of the instantaneous frequency, is straightforward from the technical point of view. Such a chirp arises around the maximum of a Gaussian light pulse, where the temporal pulse envelope can be approximated with a quadratic function of time.

It is physically instructive to consider the compression of chirped light pulses in the time domain. Since the frequency of a chirped pulse changes from its leading edge to its trailing edge, dispersion of our compressor should be designed in such a way as to slow down the leading edge of the pulse with respect to the trailing edge of the pulse.

In other words, the group velocities for the frequencies propagating with the leading edge of the pulse should be lower than the group velocities for the frequencies propagating with the trailing edge of the pulse. This can be achieved by designing a dispersive element with the required sign of dispersion and appropriate dispersion relation. Systems of diffraction gratings and, recently, multilayer chirped mirrors (see the review [4]) are now widely used for the purposes of pulse compression. In certain regimes of pulse propagation, self-phase modulation and pulse compression may take place in the same medium.

3.1.3 Cross-phase modulation. Cross-phase modulation is a result of nonlinear-optical interaction of at least two physically distinguishable light pulses (i.e., pulses with different frequencies, polarizations, mode structures, etc.) related to the phase modulation of one of the pulses (a probe pulse) due to the change in the refractive index of the medium induced by another pulse (a pump pulse).

The cross-action of a pump pulse with a frequency ω_1 on a probe pulse with a frequency ω_2 gives rise to a phase shift of the probe pulse, which can be written as [65, 66]

$$\Phi_{\mathrm{XPM}}(\eta, z) = \frac{3\pi\omega_2^2}{c^2 k_2}\, \chi^{(3)}(\omega_\mathrm{s};\omega_\mathrm{s},\omega_\mathrm{p},-\omega_\mathrm{p}) \times \int_0^z \left| A_\mathrm{p}\left(\eta - \frac{\zeta}{\sigma}\,, 0\right)\right|^2 \mathrm{d}\zeta\,, \qquad (7)$$

where $\chi^{(3)}(\omega_\mathrm{s};\omega_\mathrm{s},\omega_\mathrm{p},-\omega_\mathrm{p})$ is the third-order nonlinear-optical susceptibility of the medium; $1/\sigma = 1/u_1 - 1/u_2$; u_1 and u_2 are the group velocities of the pump and probe pulses, respectively; and k_2 is the wave number of the pump pulse. Taking the time derivative of the nonlinear phase shift, we

arrive at the following expression for the frequency deviation of the probe pulse:

$$\delta\omega_{\mathrm{XPM}}(\eta,z) = -\frac{3\pi\omega_2^2}{c^2k_2}\,\chi^{(3)}(\omega_\mathrm{s};\omega_\mathrm{s},\omega_\mathrm{p},-\omega_\mathrm{p}) \times \sigma\left[\left|A_\mathrm{p}(\eta,0)\right|^2 - \left|A_\mathrm{p}\left(\eta-\frac{z}{\sigma}\,,0\right)\right|^2\right]. \quad (8)$$

Similar to self-phase modulation, cross-phase modulation can be employed for pulse compression. The dependence of the chirp of the probe pulse on the pump pulse intensity can be used to control parameters of ultrashort pulses [41, 42, 50]. Cross-phase modulation also opens the way to study the dynamics of ultrafast nonlinear processes, including multiphoton ionization, and to characterize ultrashort light pulses through phase measurements on a short probe pulse.

3.1.4 Multiwave mixing and high-order harmonic generation. Coherent multiwave mixing and high-order harmonic generation play an important role in the nonlinear optics of hollow fibers, allowing high efficiencies of frequency conversion and high sensitivities of methods of coherent nonlinear spectroscopy to be achieved. In the case when pump pulses with frequencies ω_1 and ω_2 are coupled into a fiber, coherent multiwave mixing leads to the generation of new spectral components with frequencies $\omega_{mn} = m\omega_1 \pm n\omega_2$, where m and n are integers. The cases of $m = 0$ and $n = 0$ then correspond to the generation of nth- and mth-order harmonics of radiation with frequencies ω_1 and ω_2.

Due to the central symmetry of gas media, even-order nonlinear processes are usually characterized by much lower efficiencies as compared to odd-order nonlinear processes [29]. However, even-order nonlinear-optical processes may take place as a result of inhomogeneities in a medium or in the light field violating the central symmetry of the problem. This may be the case, for example, in the regime of gas ionization.

Specific features of multiwave mixing related to the guided-wave propagation of ultrashort pulses in a gas filling a hollow fiber include large interaction lengths, the presence of the waveguide dispersion component, and multimode regimes of wave mixing. All these physical factors have to be taken into consideration for the optimization of nonlinear-optical frequency conversion and short-pulse formation in hollow fibers. In particular, the increase in the wave-mixing length may improve the efficiency of frequency conversion only when the nonlinear process is phase-matched on the spatial scale on the order of the fiber length. These factors will be considered in greater detail in Sections 6 and 7 of this review.

3.1.5 Stimulated Raman scattering. Stimulated Raman scattering (SRS) is one of the most extensively used and intensely studied phenomena in nonlinear optics. The SRS effect arises due to the modulation of laser radiation by molecular vibrations in a medium. In contrast to spontaneous light scattering, stimulated scattering involves molecular modes excited and phased by light in a large volume of a medium, which results in the generation of highly intense and well-directed radiation.

Multiple Stokes and anti-Stokes components produced by SRS are separated by the frequency Ω of molecular vibrations. A simple model of the SRS process interprets this phenomenon as a result of harmonic phase modulation of a light pulse with the frequency Ω of molecular vibrations. The spectrum of a laser pulse propagating in a Raman-active medium under these conditions becomes dressed with Stokes and anti-Stokes components. The equidistant frequency components arising in the spectrum of such a pulse can be employed, as shown in Refs [13–16] (see Section 8 of this review), for the synthesis of ultrashort light pulses.

3.1.6 Effects related to gas ionization. The goals of nonlinear-optical experiments performed with the use of hollow fibers usually involve efficient frequency conversion or formation of ultrashort pulses. Sometimes, high-order optical nonlinearities are employed for this purpose, and laser pulses with sufficiently high power densities can be coupled into a fiber. Under these conditions, ionization effects may have a considerable influence on both dispersion and nonlinear-optical properties of the gas filling the fiber. If the collision frequency in the plasma produced as a result of this ionization process is much lower than the frequency of optical radiation, then the nonlinear additive to the refractive index of the gas associated with plasma electrons is given by

$$\Delta n = -\frac{\omega_\mathrm{p}^2}{2\omega^2}\,,$$

where $\omega_\mathrm{p}^2 = 4\pi e^2 N_\mathrm{e}/m$ is the plasma frequency, e is the electron charge, N_e is the electron plasma density, and m is the electron mass.

Dynamic variations in optical properties of the gas accompanying the propagation of a short pulse through a hollow fiber, giving rise, in particular, to the nonlinear additive to the refractive index of the gas, change phase and group-velocity matching (see Section 7.3 of this review) and may result in the temporal and spatial self- and cross-action of short light pulses. These phenomena, as shown in Ref. [59], can also be employed to produce ultrashort pulses.

3.2 Synthesis of ultrashort pulses through the generation of phase-locked equidistant spectral components: general concepts

In this section, we will consider the general physical principles of the synthesis of ultrashort pulses through the generation of phase-locked equidistant spectral components. This idea underlies a rapidly growing direction of research aimed at the formation of few-femtosecond, subfemtosecond, and attosecond pulses. Two possibilities of generating such spectral components are now actively studied. One of two ways leading beyond the femtosecond range is based on high-order harmonic generation. The other approach involves multiple Raman sideband generation through SRS (see Section 8). It seems appropriate in this context to qualitatively illustrate the basic idea of ultrashort pulse synthesis with the use of this method.

Let us consider the total electric field of a set of N equidistant spectral components with amplitudes A_n, phases φ_n, and frequencies $\omega_n = \omega_0 + n\,\delta\omega$ $(n = 1, 2, \ldots, N)$, where $\delta\omega$ is the intermode interval:

$$E(t) = \sum_{n=1}^{N} A_n \cos(\omega_n t + \varphi_n)\,. \quad (9)$$

Suppose now that all the spectral components have equal amplitudes and phases. Then, calculating the sum in Eqn (9),

we arrive at the following expression for the radiation intensity:

$$I(t) = I_0 \frac{\sin^2(N\delta\omega\, t/2)}{\sin^2(\delta\omega\, t/2)}\,, \tag{10}$$

where I_0 is the intensity of a single mode.

As can be seen from Eqn (10), the time dependence of the total radiation intensity in the case under study has a form of a sequence of pulses with the time interval between the pulses equal to $\Delta t = 2\pi/\delta\omega$ and the duration of pulses given by $\tau = 2\pi/N\,\delta\omega$. Thus, the phase-locking of equidistant spectral components is one of the key conditions for synthesizing trains of atto- and subfemtosecond pulses. This condition should be satisfied regardless of whether equidistant spectral components were produced through high-order harmonic generation or through stimulated Raman scattering. The ways to phase-lock and phase-match high-order harmonics and multiple Raman sidebands will be considered in greater detail in Sections 7 and 8 of this review.

4. Generation of ultrashort pulses using self-phase modulation in a gas-filled hollow fiber

Self-phase modulation in gas-filled hollow fibers is one of the key effects allowing the generation of high-power ultrashort light pulses [8, 9]. When optimizing hollow-fiber compressors of light pulses, it is important to remember that waveguide modes of hollow fibers are characterized by considerable optical losses, related to the nature of waveguiding of optical radiation in hollow fibers. Therefore, the analysis of the influence of optical losses on nonlinear-optical interactions in hollow fibers is very important for the optimization of parameters of hollow fibers employed to produce ultrashort light pulses [52, 53].

In this section, we will analyze the equation of self-phase modulation of a short laser pulse in leaky modes of a gas-filled hollow fiber. We will present a simple, but physically very instructive analytical solution to this equation, which reveals the main features of SPM under these conditions and allows the influence of waveguide losses to be included in the analysis aimed at optimizing pulse compressors based on gas-filled hollow fibers.

4.1 Parameters of waveguide modes of hollow fibers

Consider a light pulse with a transverse distribution corresponding to the EH_{1n} mode of a hollow fiber propagating along the z-axis chosen along the axis of a hollow fiber filled with a gas with an inertialess Kerr nonlinearity:

$$E = \frac{1}{2}\, f^n(\rho)\, A^n(\eta^n, z)\, \exp\left[-\mathrm{i}\omega t + \left(\mathrm{i}K^n - \frac{\alpha^n}{2}\right)z\right] + \text{c.c.}\,, \tag{11}$$

where ω is the central frequency of the light pulse; $f^n(\rho)$, $A^n(\eta^n, z)$, K^n, and α^n are the transverse field distribution, the slowly varying pulse envelope, the propagation constant, and the attenuation coefficient corresponding to the EH_{1n} mode of the hollow fiber; $\eta^n = (t - z/v_n)/\tau$ is the time (in the frame of reference running with the pulse) normalized to the pulse duration τ; and v_n is the group velocity of the pulse.

The z-dependence for the guided modes of a hollow fiber involves a factor $\exp(\mathrm{i}K^n z)$, similar to the case of a plane wave. However, the propagation constant K^n differs from the wave number $k = \omega n/c$ of a light wave in a gas with a refractive index n (see Section 4) because of a nonzero transverse component of the wave number in guided modes, resulting from a multiple reflection of radiation from waveguide walls.

We assume that the attenuation coefficient for the considered light pulse is small, and the wavelength is much less than the inner radius of the hollow fiber a:

$$\frac{\omega a}{c} \gg 1\,, \tag{12}$$

$$\left|\frac{K^n c}{\omega n_1(\omega)} - 1\right| \ll 1\,, \tag{13}$$

where $n_1(\omega)$ is the refractive index of the gas filling the fiber at the frequency ω. Under these conditions, we can employ approximate analytical solutions for the transverse field distribution and propagation constants of an electromagnetic field in a hollow fiber.

In the case of EH_{1n} modes of a hollow fiber, we have [54, 55]

$$f^n(\rho) = J_0\left(\frac{u^n \rho}{a}\right). \tag{14}$$

Here, $J_0(x)$ is the zeroth-order Bessel function and u^n is the eigenvalue of the characteristic equation for the EH_{1n} mode. Propagation constants and attenuation coefficients are then given by [54]:

$$K^n \approx \frac{\omega n_1(\omega)}{c}\left\{1 - \frac{1}{2}\left[\frac{u^n c}{a\omega n_1(\omega)}\right]^2\right\}, \tag{15}$$

$$\alpha^n \approx \frac{2}{a n_1(\omega)}\left(\frac{u^n c}{a\omega}\right)^2 \frac{\varepsilon_2(\omega) + n_1^2(\omega)}{2n_1^2(\omega)\left[\varepsilon_2(\omega) - n_1^2(\omega)\right]^{1/2}}\,, \tag{16}$$

where $\varepsilon_2(\omega)$ is the dielectric function of fiber walls at the frequency ω.

As can be seen from Eqn (15), the propagation constant in a hollow fiber differs from the wave number describing the propagation of a wave in a gas medium with the refractive index $n_1(\omega)$. This circumstance suggests the way to achieve phase and group-velocity matching for nonlinear-optical processes in hollow fibers by using the dispersion of guided modes to compensate for the material dispersion of the gas filling the fiber.

4.2 Equation of self-phase modulation and its solution

Using a procedure similar to that described in Ref. [29], we derive the following equation for the slowly varying pulse envelope:

$$\frac{\mathrm{d}A^n}{\mathrm{d}z} + \frac{\alpha^n}{2}\, A^n = \mathrm{i}\gamma^n A^n |A^n|^2\,, \tag{17}$$

where the nonlinear coefficient γ^n can be expressed in terms of the nonlinear-optical cubic susceptibility with the relevant frequency arguments,

$$\gamma^n = \frac{3\pi\omega^2}{2K^n c^2}\, \chi^{(3)}(\omega; \omega, -\omega, \omega)\, \frac{\iint\left[f^n(\rho)\right]^4 \rho\, \mathrm{d}\rho\, \mathrm{d}\theta}{\iint\left[f^n(\rho)\right]^2 \rho\, \mathrm{d}\rho\, \mathrm{d}\theta}\,. \tag{18}$$

Solving Eqn (17), we arrive at the following expressions for the amplitude and the phase of the pulse:

$$A^n(\eta^n, z) = A_0^n(\eta^n) \exp\left[i\varphi(\eta^n, z) - \frac{1}{2}\alpha^n z\right], \tag{19}$$

$$\varphi(\eta^n, z) = \frac{\gamma^n}{\alpha^n}\left|A_0^n(\eta^n)\right|^2\left[1 - \exp\left(-\alpha^n z\right)\right]. \tag{20}$$

Formulas (19) and (20) are very instructive, as they provide a clear physical understanding of how the amplitude and the phase of a self-phase-modulated pulse evolve in space, revealing the role of waveguide losses in the SPM of a short pulse in a hollow fiber.

4.3 Amplitude and chirp evolution

Let us introduce a parameter β characterizing the chirp of a light pulse:

$$\beta = \frac{\partial^2\varphi(\eta^n, z)}{(\partial\eta^n)^2}. \tag{21}$$

Substituting Eqn (20) into Eqn (21), we derive

$$\beta(\eta^n, z) = \frac{\gamma^n}{\alpha^n}\frac{\partial^2\left|A_0^n(\eta^n)\right|^2}{(\partial\eta^n)^2}\left[1 - \exp\left(-\alpha^n z\right)\right]. \tag{22}$$

As can be seen from Eqns (19), (20), and (22), the chirp parameter β first increases and then saturates at some level determined by the attenuation coefficient α. The amplitude of the chirped pulse under these conditions monotonically decreases as a function of z (Fig. 1).

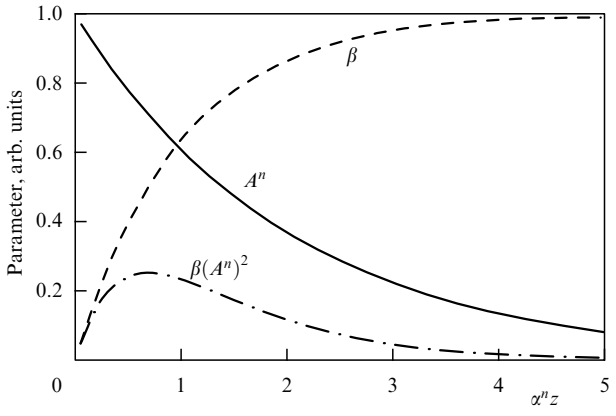

Figure 1. Chirp parameter β, pulse amplitude A^n, and the parameter $\beta(A^n)^2$ as functions of the normalized coordinate $\alpha^n z$ for a light pulse propagating in a leaky mode of a hollow fiber.

4.4 The amplitude of a compressed pulse

Let us estimate the amplitude of a pulse transmitted through a hollow fiber after chirp compensation. Provided that SPM puts a considerable chirp on the pulse,

$$\beta \gg \tau^{-2}, \tag{23}$$

the ratio of the power of the pulse with compensated chirp to the initial pulse power is proportional to β [56], which implies that the power of the pulse after chirp compensation is proportional to the product of the chirp parameter and the pulse amplitude squared:

$$P_c \propto \beta(A^n)^2. \tag{24}$$

As can be seen from Fig. 1, the maximum power of a compressed pulse is achieved with some fiber length L_{opt}, depending on the inner radius of the hollow fiber [see Eqns (19), (20), and (22)]. The expressions derived above also allow the estimation of the dependence of the maximum power of compressed pulse P_{max} on the inner radius of a hollow fiber with an optimal length L_{opt}. When the intensity of a light pulse is fixed, Eqns (19), (20), (22), and (24) yield

$$P_{max} \propto a^5. \tag{25}$$

In a situation when the pulse power is fixed, the light intensity in a hollow fiber is proportional to a^{-2}, which implies that $A_0^n \sim a^{-1}$. Then, using Eqns (19), (20), (22), and (24), we find that

$$P_{max} \sim a. \tag{26}$$

Thus, the power of a compressed pulse can be increased with both fixed pulse power and fixed light intensity by using fibers with larger inner diameters. Apparently, limitations on the increase in the power of a compressed pulse in this case may be mainly associated with the excitation of higher order waveguide modes in a hollow fiber.

Thus, we have presented a simple analytical solution to the equation governing the self-phase modulation of a light pulse in leaky modes of a hollow fiber, which reveals the main features of the SPM process in a hollow fiber and permits optimization of parameters of hollow-fiber pulse compressors. Analysis of this solution shows that the increase of the chirp parameter of a self-phase-modulated pulse in a hollow fiber saturates at some level determined by the attenuation coefficient of the waveguide mode. The amplitude of the chirped pulse under these conditions monotonically decreases as a function of the propagation length of the pulse in the fiber.

It should be mentioned that, as a short laser pulse propagates through a hollow fiber and its spectrum becomes broader and broader due to self-phase modulation, group-velocity dispersion effects become more and more important. Analysis of such effects requires the inclusion of higher order dispersion terms into the equation for the complex amplitude of a light pulse, and the first-order dispersion theory approximation becomes inapplicable.

5. Cross-phase modulation and control of ultrashort light pulses in a hollow fiber

Cross-phase modulation provides an opportunity to control parameters of short pulses of short-wavelength radiation produced through nonlinear-optical interactions in gas-filled hollow fibers [41, 42]. In particular, in the case of third-harmonic generation in a hollow fiber, the fundamental pulse, efficiently interacting with its third harmonic and, at the same time, experiencing noticeable self-phase modulation, leads to the cross-phase modulation of the third-harmonic pulse [41, 42].

Similar SPM and XPM phenomena have been also observed in experiments on third-harmonic generation in the field of ultrashort laser pulses leading to the ionization

of air [57, 58], where the temporal self-action of light pulses was accompanied by the self-defocusing of fundamental radiation due to the induced density profile of plasma electrons. Theoretical analysis performed in Ref. [59] has demonstrated that SPM due to plasma nonlinearity under conditions of ionization in a hollow waveguide makes it possible to produce light pulses with a linear chirp, which can be efficiently compensated with a dispersive delay line (the influence of ionization effects on harmonic generation in hollow fibers has been also considered in Refs [60, 61]).

Let us consider third-harmonic generation in a hollow optical fiber filled with a gas medium with a third-order nonlinearity. To analyze this process, we will employ the approximation of slowly varying envelopes, assuming that the duration of light pulses is large as compared with a cycle of the optical field. Physically instructive expressions governing third-harmonic generation in a hollow fiber that take into account SPM and XPM can be derived in the case when consideration can be restricted to first-order dispersion effects. Such an approximation is widely used in guided-wave optics [62–67], as it may provide a qualitative understanding of the main features of nonlinear-optical processes. The results obtained within the framework of this approximation can be then used, in particular, as an initial guess for more detailed and accurate, but less physically transparent, numerical simulations.

Let us represent the pulses of fundamental radiation (pump) and its third harmonic propagating along the z-axis in a hollow fiber filled with a gas with an instantaneous Kerr nonlinearity (where dispersion of the second and higher orders can be neglected) in the following form:

$$\mathbf{E}_\mathrm{p} = \frac{1}{2} f_\mathrm{p}^{n'n}(\boldsymbol{\rho})\, \mathbf{e}_\mathrm{p}^{n'n} A^{n'n}(t,z) \exp\left[-\mathrm{i}(\omega t - K_\mathrm{p}^{n'n} z)\right] + \text{c.c.}, \quad (27)$$

$$\mathbf{E}_\mathrm{h} = \frac{1}{2} f_\mathrm{h}^{m'm}(\boldsymbol{\rho})\, \mathbf{e}_\mathrm{h}^{m'm} B^{m'm}(t,z) \exp\left[-\mathrm{i}(3\omega t - K_\mathrm{h}^{m'm} z)\right] + \text{c.c.}, \quad (28)$$

where ω is the central frequency of fundamental radiation; the indices 'p' and 'h' correspond to the pumping and third-harmonic pulses, respectively; $f_\mathrm{p}^{n'n}(\boldsymbol{\rho})$ and $f_\mathrm{h}^{m'm}(\boldsymbol{\rho})$ are the transverse distributions of the field in the fundamental beam and the third harmonic in a hollow fiber that correspond to the relevant eigenmodes of the hollow fiber with indices n', n and m', m, respectively; $K_\mathrm{p}^{n'n}$ and $K_\mathrm{h}^{m'm}$ are the propagation constants of the fundamental pulse and the third harmonic corresponding to the relevant eigenmodes of the hollow fiber [54, 55]; $A^{n'n}(t,z)$ is the slowly varying amplitude of the fundamental pulse (we assume that a definite waveguide mode is excited at the fundamental frequency); $B^{m'm}(t,z)$ is the slowly varying amplitude of the third harmonic (indices specifying the transverse mode of the corresponding pumping beam are omitted to simplify notation); and $\mathbf{e}_\mathrm{p}^{n'n}$ and $\mathbf{e}_\mathrm{h}^{m'm}$ are the unit polarization vectors of fundamental radiation and the third harmonic, respectively.

When inequalities (12) and (13) are satisfied for the fundamental frequency and its third harmonic, we can employ approximate analytical solutions for the transverse distribution of the field and propagation constants in a hollow fiber [54]. In particular, for EH_{1m} modes of a hollow fiber, we have

$$f_l^{1m}(\boldsymbol{\rho}) \equiv f_l^m(\boldsymbol{\rho}) = J_0\left(\frac{u_m \rho}{a}\right). \quad (29)$$

Here, $J_0(x)$ is the zeroth-order Bessel function, u_m is the eigenvalue of the EH_{1m} mode ($l = \mathrm{p}, \mathrm{h}$), a is the inner radius of the hollow fiber, and

$$K_l^{1m} \equiv K_l^m \approx \frac{\omega_l n_1(\omega_l)}{c} \times \left[1 - \left(\frac{u_m c}{a\omega_l n_1(\omega_l)}\right)^2 \left(\frac{1}{2} + \frac{c}{a\omega_l}\,\mathrm{Im}\,\mu(\omega_l)\right)\right], \quad (30)$$

where

$$\mu(\omega_l) = \frac{\varepsilon_2(\omega_l) + n_1^2(\omega_l)}{2n_1^2(\omega_l)\left[\varepsilon_2(\omega_l) - n_1^2(\omega_l)\right]^{1/2}}$$

for EH modes and $\varepsilon_2(\omega_l)$ is the dielectric constant of the walls of the fiber at the frequency ω_l.

The slowly varying amplitudes $A^n(z,t) \equiv A^{1n}(z,t)$ and $B^m(z,t) \equiv B^{1m}(z,t)$ of the pumping pulse and the third harmonic are governed by the equations

$$\left(\frac{\partial}{\partial t} + \frac{1}{v_\mathrm{p}^n}\frac{\partial}{\partial z}\right) A^n = \mathrm{i}\tilde{\gamma}_1^n A^n |A^n|^2, \quad (31)$$

$$\left(\frac{\partial}{\partial t} + \frac{1}{v_\mathrm{h}^m}\frac{\partial}{\partial z}\right) B^m = \mathrm{i}\tilde{\beta}^{mn}(A^n)^3 \exp(-\mathrm{i}\Delta k^{mn} z) + 2\mathrm{i}\tilde{\gamma}_2^{mn} B^m |A^n|. \quad (32)$$

Here, v_p^n and v_h^m are the group velocities of the fundamental and third-harmonic pulses, respectively, and

$$\Delta k^{mn} = K_\mathrm{h}^m - 3K_\mathrm{p}^n \approx \Delta k_0 + \Delta k_\mathrm{w}^{mn} \quad (33)$$

is the phase mismatch that includes the waveguide dispersion, where

$$\Delta k_0 = \frac{\omega_\mathrm{h}}{c}\left[n_1(\omega_\mathrm{h}) - n_1(\omega_\mathrm{p})\right],$$

$$\Delta k_\mathrm{w}^{mn} = \frac{c}{\omega_\mathrm{p}}\left[3\left(\frac{u_\mathrm{p}^n}{a}\right)^2 - \frac{1}{3}\left(\frac{u_\mathrm{h}^m}{a}\right)^2\right]$$

are the components of the phase mismatch due to gas and waveguide dispersion, respectively. The total phase mismatch can be represented as a sum of two components in the case when the inequality $n_1(\omega_l) - 1 \ll 1$ is satisfied.

The nonlinear coefficients $\tilde{\gamma}_1^m$, $\tilde{\gamma}_2^{mn}$, and $\tilde{\beta}^{mn}$ can be expressed in terms of the nonlinear-optical cubic susceptibilities with the relevant frequency arguments:

$$\tilde{\gamma}_1^n = \frac{3\pi\omega^2}{2K_\mathrm{p}^n c^2}\, \mathbf{e}_\mathrm{p}^{n*}\, \hat{\chi}^{(3)}(\omega;\omega,-\omega,\omega)\, \mathbf{e}_\mathrm{p}^n \mathbf{e}_\mathrm{p}^{n*} \mathbf{e}_\mathrm{p}^n \times \frac{\iint \left[f_\mathrm{p}^n(\boldsymbol{\rho})\right]^4 \rho\, \mathrm{d}\rho\, \mathrm{d}\theta}{\iint \left[f_\mathrm{p}^n(\boldsymbol{\rho})\right]^2 \rho\, \mathrm{d}\rho\, \mathrm{d}\theta}, \quad (34)$$

$$\tilde{\gamma}_2^{mn} = \frac{27\pi\omega^2}{2K_\mathrm{h}^m c^2}\, \mathbf{e}_\mathrm{h}^{m*}\, \hat{\chi}^{(3)}(3\omega;3\omega,-\omega,\omega)\, \mathbf{e}_\mathrm{h}^m \mathbf{e}_\mathrm{p}^{n*} \mathbf{e}_\mathrm{p}^n \times \frac{\iint \left[f_\mathrm{h}^m(\boldsymbol{\rho})\right]^2 \left[f_\mathrm{p}^n(\boldsymbol{\rho})\right]^2 \rho\, \mathrm{d}\rho\, \mathrm{d}\theta}{\iint \left[f_\mathrm{h}^m(\boldsymbol{\rho})\right]^2 \rho\, \mathrm{d}\rho\, \mathrm{d}\theta}, \quad (35)$$

$$\tilde{\beta}^{mn} = \frac{9\pi\omega^2}{2K_\mathrm{h}^m c^2}\, \mathbf{e}_\mathrm{h}^{m*}\, \hat{\chi}^{(3)}(3\omega;\omega,\omega,\omega)\, \mathbf{e}_\mathrm{p}^n \mathbf{e}_\mathrm{p}^{n*} \mathbf{e}_\mathrm{p}^n \times \frac{\iint f_\mathrm{h}^m(\boldsymbol{\rho}) \left[f_\mathrm{p}^n(\boldsymbol{\rho})\right]^3 \rho\, \mathrm{d}\rho\, \mathrm{d}\theta}{\iint \left[f_\mathrm{h}^m(\boldsymbol{\rho})\right]^2 \rho\, \mathrm{d}\rho\, \mathrm{d}\theta}. \quad (36)$$

Equations (31) and (32) are similar to the equations that describe third-harmonic generation in a gas medium with SPM and XPM within the framework of the plane-wave approximation. The nonlinear term on the right-hand side of Eqn (31) describes the SPM effect. The first term on the right-hand side of Eqn (32) describes the third-order polarization of a medium responsible for third-harmonic generation and XPM of the third harmonic due to SPM of the fundamental pulse. The second term on the right-hand side of this equation is responsible for XPM due to the modulation of the refractive index at the frequency of the third harmonic by the fundamental pulse.

In writing Eqn (32), we assumed that the third-harmonic pulse is rather weak, and self-phase modulation for this pulse is negligible. However, in contrast to the plane-wave approximation, Eqns (31) and (32) take into account the influence of a waveguide through propagation constants (30), group velocities of the pumping pulse and the third harmonic, and nonlinear coefficients (34)–(36), which explicitly involve factors sensitive to the transverse distributions of the pumping and third-harmonic fields for the relevant waveguide modes. In particular, the phase mismatch, which is involved in Eqn (32) and which determines the efficiency of third-harmonic generation, depends not only on the gas dispersion, but also on the dispersion of waveguide modes. As pointed out in Refs [40–42], this circumstance provides an opportunity to improve phase-matching conditions for a certain pair of transverse modes of fundamental radiation and the third harmonic.

Solving the set of equations (31) and (32), we derive the following expressions for the amplitudes of the fundamental pulse and the third harmonic:

$$A^n(\eta_p^n, z) = A_0^n(\eta_p^n)\exp\left[i\tilde{\gamma}_1^n\left|A_0^n(\eta_p^n)\right|^2 z\right], \tag{37}$$

$$\begin{aligned} B^m(\eta_h^m, z) = {} & i\tilde{\beta}^{mn}\exp\left[2i\tilde{\gamma}_2^{mn}\int_0^z \left|A_0^n(\eta_h^m + \zeta^{mn}z')\right|^2 dz'\right] \\ & \times \int_0^z dz'\left[A_0^n(\eta_h^m + \zeta^{mn}z')\right]^3 \\ & \times \exp\left[-i\Delta k^{mn}z' + 3i\tilde{\gamma}_1^m\left|A_0^n(\eta_h^m + \zeta^{mn}z')\right|^2 z' \right. \\ & \left. - 2i\tilde{\gamma}_2^{mn}\int_0^{z'}\left|A_0^n(\eta_h^m + \zeta^{mn}z'')\right|^2 dz''\right], \end{aligned} \tag{38}$$

where $\eta_l^m = (t - z/v_l^m)/\tau$ is the time in the frame of reference running with one of the pulses ($l = p, h$) normalized to the duration τ of the incident pulse and $\zeta^{mn} = (1/v_h^m - 1/v_p^n)\tau^{-1}$. Since we restrict our consideration to the first order of dispersion theory, the fundamental pulse (37) propagates in a fiber without changing its waveform, $A^n(\eta_p^n, z) = A_0^n(\eta_p^n)$, where $A_0^n(\eta_p^n)$ is the envelope of the fundamental pulse at the input of the fiber.

The results of numerical simulations presented in Fig. 2 show that the third-harmonic pulse experiences phase modulation due to XPM, and the spectrum of this pulse features considerable broadening even as compared with the pump pulse, which is subject to SPM. Due to this effect, the third-harmonic pulse can be efficiently compressed through the compensation of a linear chirp (Fig. 3). With the growth in the pump power, as can be seen from Fig. 4, the chirp of the third-harmonic pulse and its spectral width increase, which makes it possible to obtain sufficiently short pulses at the output of a compressor. It should be noted, however, that the increase in the pump power may give rise to distortions in the waveform of the third-harmonic pulse.

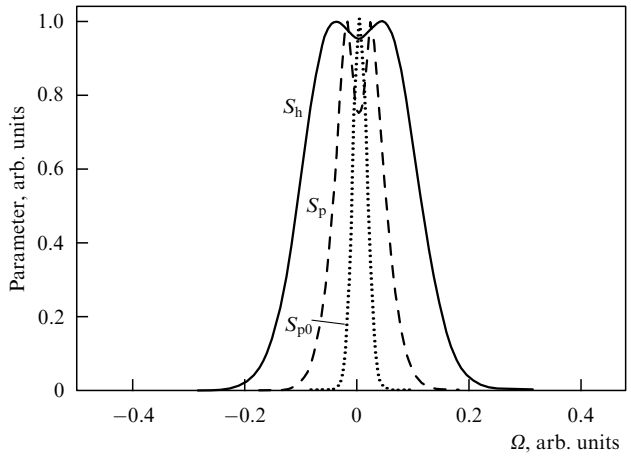

Figure 2. Spectrum of the third harmonic emitted into the EH_{11} mode at the output of a fiber, S_h, and the pumping pulse at the output, S_p, and at the input, S_{p0}, of the fiber for $p = 0.536$ atm and $P_{p0} = 1$ GW.

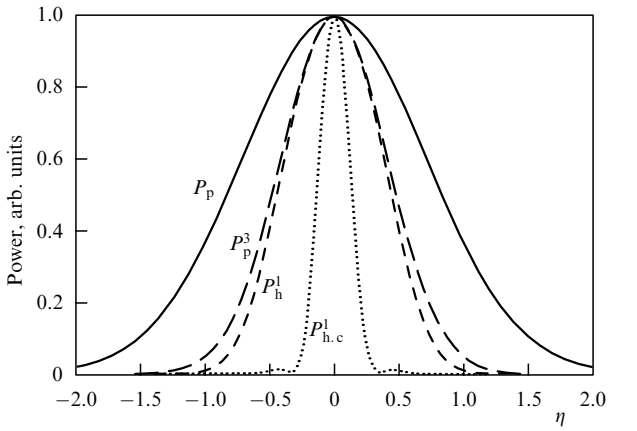

Figure 3. Normalized pump power P_p, the cube of the pump power P_p^3, and the power of the EH_{11} mode of the third harmonic at the output of the fiber, P_h^1, and upon the compensation of a linear chirp, $P_{h.c}^1$, as functions of the running time η for $p = 0.536$ atm and $P_{p0} = 2$ GW.

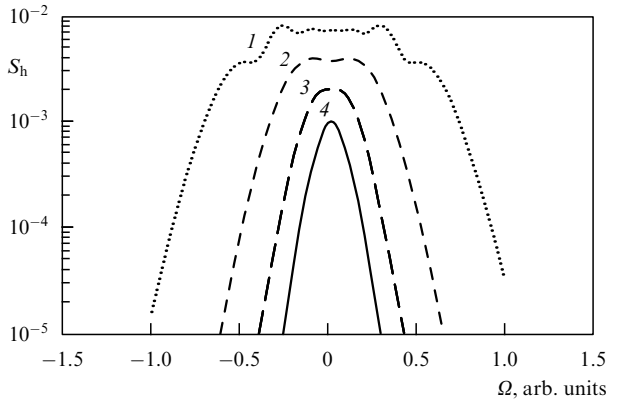

Figure 4. Spectrum of the third-harmonic pulse emitted into the EH_{11} mode at the output of a hollow fiber S_h for (*1*) $P_{p0} = 4$ GW and $p = 0.549$ atm, (*2*) $P_{p0} = 2$ GW and $p = 0.536$ atm, (*3*) $P_{p0} = 1$ GW and $p = 0.545$ atm, and (*4*) $P_{p0} = 0.5$ GW and $p = 0.549$ atm.

Thus, cross-phase modulation, which accompanies third-harmonic generation in a hollow fiber, allows one to control

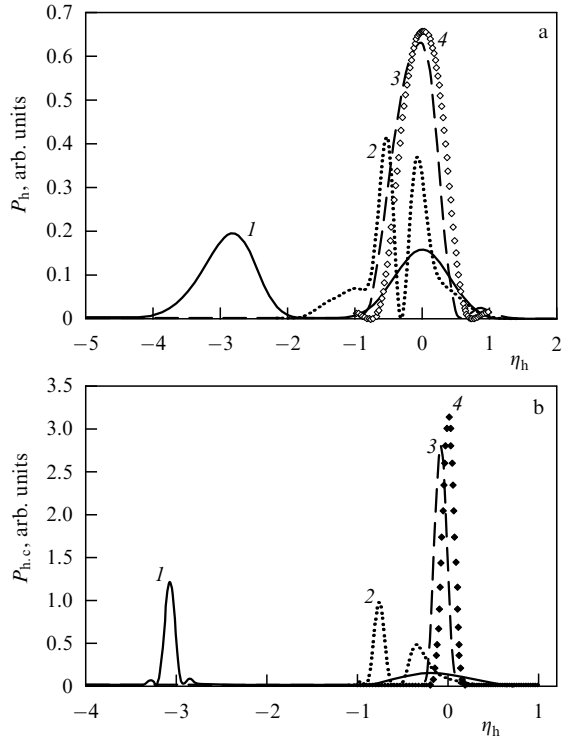

Figure 5. Power of the fundamental mode of the third-harmonic pulse $P_h \equiv P_h^1$ at the output of a hollow fiber (a) and upon the compensation of a linear chirp (b) as a function of running time η_h for $p = 0.52$ atm and $P_{p0} = 4$ GW with the pump pulse duration 2τ equal to 25 fs (*1*), 100 fs (*2*), and 800 fs (*3*) and in the case when the walk-off of the pump and third-harmonic pulses is neglected (*4*).

the chirp of the third harmonic by varying the amplitude of the pump pulse and parameters (pressure and dispersion) of the gas filling the fiber. This effect provides an opportunity to produce light pulses with a tripled frequency and controllable pulse duration.

Generally, group-delay effects may have a considerable influence on third-harmonic generation with short light pulses in a hollow fiber. As revealed by the envelopes of the power of the pump pulse and the fundamental mode of the third harmonic at the output of a fiber (Fig. 5a), due to the walk-off of the pumping pulse and the third harmonic, the third-harmonic pulse first becomes longer (curve *2* in Fig. 5a, where the walk-off of the fundamental pulse and the third harmonic within the fiber length is equal to $\eta_h \equiv \eta_h^1 = 0.8$) and then (with a further decrease in the duration of the pump pulse) splits into two spikes (curve *1* in Fig. 5a, where the walk-off of the fundamental pulse and the third harmonic within the fiber length is equal to $\eta_h = 3$).

In the latter case, the right-hand spike in Fig. 5a is produced through third-harmonic generation within an area with a length on the order of the coherence length $l_{ph}^{11} = 1/\Delta k^{11}$ near the input end of the fiber, whereas the left-hand spike emerges from third-harmonic generation in an analogous area near the output end of the fiber. The power of the third harmonic produced in the central part of the fiber is negligibly small compared with the third-harmonic signal generated near the ends of the fiber. This effect can be easily explained with the use of Eqn (38).

Indeed, assuming that the walk-off length meets the inequality $l_w \ll L$, letting the upper integration limit in Eqn (38) tend to infinity, and taking into account that, for low pump powers, the second and third terms in the argument of the exponential are small as compared with the first term, we find that the power of the third-harmonic signal is determined by the Fourier transform of the amplitude of the pump pulse in Δk representation:

$$B^m(\eta_h^m, z) \approx \mathrm{i}\,\frac{\tilde{\beta}^m}{\zeta^{mn}} \int_0^{z/\zeta^{mn}} \mathrm{d}\eta''\,\left[A_0^n(\eta_h + \eta'')\right]^3 \times \exp\left(-\mathrm{i}\,\frac{\Delta k^{mn}}{\zeta^{mn}}\,\eta''\right).$$

Physically, the low efficiency of third-harmonic generation in the central part of the fiber is associated with a large phase mismatch between the pump pulse and the third harmonic ($\Delta k^{11}/\zeta^{11} \sim 100$ for 25-fs pulses at an argon pressure of 0.5 atm).

Importantly, the third-harmonic spike produced near the output end of the fiber experiences much stronger phase modulation and, consequently, allows a higher compression efficiency (Fig. 5b) to be achieved as compared with the third-harmonic spike generated near the input end of the fiber. This is due to the fact that, due to SPM, the pump pulse features much stronger phase modulation near the output end of the fiber than near its input end. Therefore, the third-harmonic spike generated near the output end of the fiber has a stronger phase modulation and ensures a higher efficiency of pulse compression through chirp compensation (Fig. 5b). The relevant spectra of pump and third-harmonic pulses are presented in Fig. 6. Similar to the case of a small walk-off of the pump pulse and the third harmonic, the growth in the pump power increases the spectral width of the third-harmonic pulse (Fig. 7).

Thus, under conditions of noticeable walk-off of the pump pulse and the third harmonic, the nonlinear-optical interaction of short laser pulses in a gas-filled hollow fiber becomes much more complex than in the absence of group-delay effects. However, even in this case, cross-phase modulation provides an opportunity to control parameters of third-harmonic pulses (see Fig. 7) and to produce ultrashort light pulses in the ultraviolet range.

Generation of ultrashort pulses of short-wavelength radiation using cross-phase modulation in nonlinear-optical interactions in gas-filled hollow fibers has been

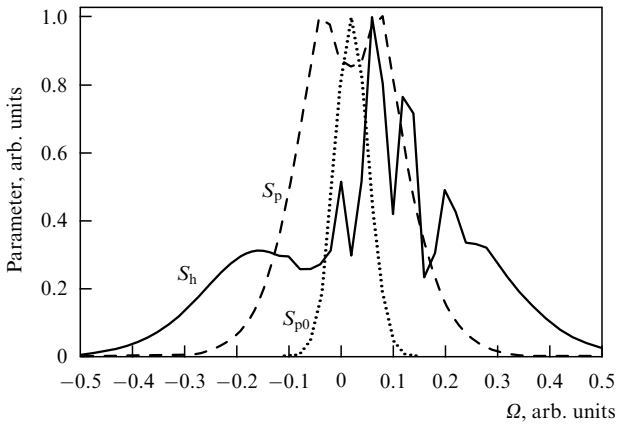

Figure 6. Spectrum of the third harmonic emitted into the EH_{11} mode at the output of a hollow fiber, S_h, and the pump pulse at the output, S_p, and at the input, S_{p0}, of the fiber for $p = 0.506$ atm, $P_{p0} = 2$ GW, and the pulse duration $2\tau = 50$ fs.

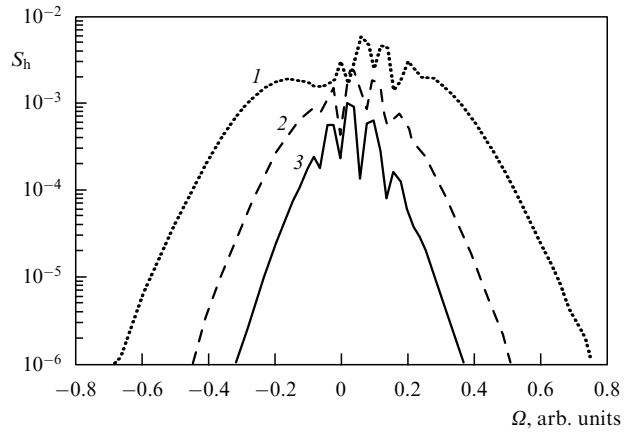

Figure 7. Spectrum of the third harmonic emitted into the EH_{11} mode at the output of a hollow fiber for $2\tau = 25$ fs and (*1*) $P_{p0} = 2$ GW and $p = 0.505$ atm, (*2*) $P_{p0} = 1$ GW and $p = 0.514$ atm, and (*3*) $P_{p0} = 0.5$ GW and $p = 0.518$ atm.

elegantly implemented by Durfee et al. [50], who investigated the process of difference-frequency generation $3\omega = 2\omega + 2\omega - \omega$, where ω is the frequency of Ti:sapphire-laser fundamental radiation (with a wavelength of 800 nm) and 2ω is the second harmonic of the fundamental frequency (with a wavelength of 400 nm). The energy of radiation generated at the frequency 3ω (the wavelength is 270 nm) at the output of the fiber was as high as 10 μJ. The efficiency of energy conversion from second-harmonic radiation into radiation with the frequency 3ω exceeded 20%. The duration of the fundamental pulse was equal to 35 fs. For low powers of the fundamental pulse, the duration of the 3ω pulse was about 20 fs.

With an increase in the power of fundamental radiation, the spectrum of 3ω radiation displayed considerable broadening due to cross-phase modulation. The use of a prism compressor allowed the authors of Ref. [50] to produce 8-fs pulses of 3ω radiation with a sufficiently high quality of pulse waveforms. The spectral width of the 3ω pulse increased with further growth in the pump power. According to the estimates of Ref. [50], the spectral broadening observed in experiments would be sufficient, with an appropriate chirp profile, to produce sub-3-fs pulses of 270-nm radiation.

6. Four-wave mixing in hollow fibers as a way to improve the sensitivity of nonlinear-optical gas-phase analysis

6.1 The diagnostic aspect of nonlinear-optical processes in hollow fibers

In this section, we will examine the potential of hollow fibers for improving the sensitivity and expanding the capabilities of coherent four-wave-mixing spectroscopy [38, 47, 48]. We will study the properties of nonlinear-optical interactions in gas-filled hollow fibers that open new avenues for numerous practical applications of hollow fibers in nonlinear optics, the optics of ultrashort pulses, and nonlinear spectroscopy.

In particular, one of the most general properties of the waveguide regime of nonlinear-optical interactions in hollow fibers is associated with the fact that the use of a hollow fiber allows high power densities of laser radiation typical of the tight-focusing regime to be achieved with an appropriate focusing of pump beams. The waveguide regime of radiation propagation under these conditions ensures the geometry of nonlinear-optical processes that is characteristic of plane-wave interaction, thus allowing the efficiency of sum-frequency generation to be considerably improved relative to nonlinear-optical interactions of tightly focused light beams in a medium with a normal dispersion.

Most of the nonlinear-optical hollow-fiber experiments performed to date were performed with the use of high-intensity femtosecond pulses (the pioneering work by Miles et al. [38] does not belong to this class of experiments, but this work does not deal with sum-frequency generation processes). The prohibition on third-harmonic generation and sum-frequency generation in a gas with an initially positive dispersion in these experiments may be removed due to the ionization of the gas (such effects were observed in numerous experiments [68 – 72]) and due to the self-action of laser pulses (which was also observed experimentally, see Refs [57, 58, 73]).

The experiments presented below in this section provide direct evidence of the possibility of sum-frequency generation and optical frequency multiplication in media with a normal dispersion due to the use of the waveguide regime of nonlinear-optical interactions. Picosecond pulses of moderate intensities (the maximum intensities of laser pulses in our experiments were on the order of 10^{11} W cm^{-2}) were used for the purposes of this demonstration. No third harmonic was generated when such laser beams were tightly focused in the gas in the absence of a fiber, which indicates that the perturbation of the gas medium and the pump beams themselves do not have a considerable influence on nonlinear-optical processes. Such an approach allowed us to study the main properties of four-wave mixing (FWM) processes in the waveguide regime and to examine the ways to phase-match FWM processes under these conditions.

One of the important results of our study is the experimental demonstration of the considerable influence of higher order waveguide modes on FWM processes in hollow fibers. Investigation of FWM of picosecond pulses is also of considerable interest in the context of the possibility of using hollow fibers to improve the sensitivity of nonlinear-optical techniques for gas-phase analysis. Picosecond pulses are often a reasonable choice for stationary spectroscopic techniques, which are widely employed for various practical applications and which may often impose certain limitations on the duration of laser pulses.

6.2 Basic relations for four-wave mixing in hollow fibers

6.2.1 The amplitude of the FWM signal. In this section, we will study the specific features of FWM processes in gas-filled hollow fibers taking into consideration the influence of phase-matching effects, optical losses of hollow-fiber modes, and higher order waveguide modes. We will consider FWM processes of third-harmonic and difference-frequency generation giving rise to a signal at the frequency of the third harmonic in accordance with the following FWM schemes: $3\omega = \omega + \omega + \omega$ and $3\omega = 2\omega + 2\omega - \omega$, where ω and 2ω are the frequencies of pump pulses (fundamental radiation of the pump laser and its second harmonic). Processes of this type, as demonstrated by experiments [40], allow high efficiencies of nonlinear-optical frequency conversion to be achieved by phase-matching the light pulses involved in FWM in a hollow fiber.

Suppose that the fundamental radiation and its second harmonic (pump pulses) propagate along the z-axis of a hollow fiber with an inner radius a. We assume that the hollow fiber is filled with a gas with a cubic nonlinearity and a refractive index n. The dielectric constant of the cladding of the hollow fiber is assumed to be a real quantity meeting the condition $\varepsilon > n^2$. The fields of the pump and FWM pulses can be then represented as

$$E_1 = \frac{1}{2} f_1^q(\rho)\, A_0^q \exp\left[-\mathrm{i}\omega t + \left(\mathrm{i}K_1^q - \frac{\alpha_1^q}{2}\right)z\right] + \text{c.c.}\,, \qquad (39)$$

$$E_2 = \frac{1}{2}\sum_l f_2^l(\rho)\, B_0^l \exp\left[-2\mathrm{i}\omega t + \left(\mathrm{i}K_2^l - \frac{\alpha_2^l}{2}\right)z\right] + \text{c.c.}\,, \qquad (40)$$

$$E_3 = \frac{1}{2} f_3^m(\rho)\, C^m(z)\, \exp\left[-3\mathrm{i}\omega t + \mathrm{i}K_3^m z\right] + \text{c.c.}\,, \qquad (41)$$

where $f_1^q(\rho)$, $f_2^l(\rho)$, and $f_3^m(\rho)$ are the transverse field distributions corresponding to the EH_{1q}, EH_{1l}, and EH_{1m} hollow-fiber modes of fundamental radiation, the second harmonic, and the FWM pulse, respectively; ρ is the distance from the axis of the hollow fiber; A_0^q and B_0^l are the amplitudes of the pulses of fundamental radiation and the second harmonic at the input of the fiber; $C^m(z)$ is the slowly varying amplitude of the FWM signal; K_1^q, K_2^l, and K_3^m are the propagation constants of fundamental radiation, the second harmonic, and the FWM signal in the hollow fiber, respectively; and α_1^q and α_2^l are the attenuation coefficients for the EH_{1q} waveguide mode at the fundamental frequency and the EH_{1l} waveguide mode at the frequency of the second harmonic.

Representing the field of the second harmonic in Eqn (40) as a sum of hollow-fiber modes, we extend our analysis to FWM processes where two of the four waves have equal frequencies 2ω, but different transverse field distributions corresponding to different waveguide modes $\mathrm{EH}_{1l'}$ and $\mathrm{EH}_{1l''}$ (i.e., $l = l', l''$).

We assume that each of the waves involved in the FWM process has a small attenuation coefficient and a wavelength much less than the fiber core radius a. Inequalities (2) and (3) are then satisfied for all the frequencies under consideration, and we can employ approximate analytical solutions of Eqns (14)–(16) for the transverse field distribution, propagation constants, and attenuation coefficients of the electromagnetic field in a hollow fiber.

The equation for the slowly varying envelope of the third harmonic in a lossy hollow fiber is written as

$$\frac{\mathrm{d}}{\mathrm{d}z} C_{\mathrm{THG}}^m + \frac{\alpha_3^m}{2} C_{\mathrm{THG}}^m = \mathrm{i}\beta_{\mathrm{THG}}^{mq} (A_0^q)^3 \exp\left(-\mathrm{i}\Delta k_{\mathrm{THG}}^{mq} z - \frac{3\alpha_1^q z}{2}\right), \qquad (42)$$

where α_3^m is the attenuation coefficient for the EH_{1m} mode of the THG signal. The phase mismatch is then written as

$$\Delta k_{\mathrm{THG}}^{mn} = K_3^m - 3K_1^q \approx \Delta k_{\mathrm{THG}}^{\mathrm{g}} + \Delta k_{\mathrm{THG}}^{\prime mq}\,, \qquad (43)$$

where

$$\Delta k_{\mathrm{THG}}^{\mathrm{g}} = \frac{3\omega}{c}\left[n(3\omega) - n(\omega)\right], \qquad (44)$$

$$\Delta k_{\mathrm{THG}}^{\prime mq} = \frac{c}{2\omega a^2}\left[3(u^q)^2 - \frac{(u^m)^2}{3}\right] \qquad (45)$$

are the components of the phase mismatch due to the dispersion of the gas and waveguide dispersion, respectively [the total phase mismatch can be represented as a sum of these two components in the case when $n(\omega), n(3\omega) \approx 1$].

The nonlinear coefficient $\beta_{\mathrm{THG}}^{mq}$ can be expressed in terms of the relevant nonlinear-optical cubic susceptibility [48]:

$$\beta_{\mathrm{THG}}^{mq} = \frac{9\pi\omega^2}{2K_3^m c^2}\,\chi_{\mathrm{THG}}^{(3)}\,\frac{\iint f_3^m(\rho)\left[f_1^q(\rho)\right]^3 \rho\,\mathrm{d}\rho\,\mathrm{d}\theta}{\iint\left[f_3^m(\rho)\right]^2 \rho\,\mathrm{d}\rho\,\mathrm{d}\theta}\,, \qquad (46)$$

where $\chi_{\mathrm{THG}}^{(3)}$ is the third-order nonlinear-optical susceptibility responsible for third-harmonic generation.

Integrating Eqn (42), we derive the following expression for the amplitude of the EH_{1m} mode of the third harmonic:

$$C_{\mathrm{THG}}^m = \mathrm{i}\beta_{\mathrm{THG}}^{mq}(A_0^q)^3 \times\left\{\exp\left(-\frac{\alpha_3^m}{2}L\right) - \exp\left[\left(-\frac{3\alpha_1^q}{2} - \mathrm{i}\Delta k_{\mathrm{THG}}^{mq}\right)L\right]\right\} \times\left(\frac{\alpha_3^m - 3\alpha_1^q}{2} - \mathrm{i}\Delta k_{\mathrm{THG}}^{mq}\right)^{-1}, \qquad (47)$$

where L is the length of the gas-filled hollow fiber.

In the limiting case of low losses and zero phase mismatch, Eqn (47) is reduced to

$$C_{\mathrm{THG}}^m = \mathrm{i}\beta_{\mathrm{THG}}^{mq}(A_0^q)^3 L\,. \qquad (48)$$

Using Eqn (48), we can obtain the following estimate for the power of the third-harmonic signal:

$$P_{\mathrm{THG}} \sim P_1^3\,\frac{L^2}{a^4}\,, \qquad (49)$$

where P_1 is the power of fundamental radiation.

In the case of a difference-frequency generation process $3\omega = 2\omega + 2\omega - \omega$, involving the EH_{1q} hollow-fiber mode of fundamental radiation and $\mathrm{EH}_{1l'}$ and $\mathrm{EH}_{1l''}$ modes of the second harmonic, generating the EH_{1m} mode of the DFG signal at the frequency of the third harmonic in a lossy hollow fiber, the slowly varying envelope of the DFG signal is governed by the following equation:

$$\frac{\mathrm{d}}{\mathrm{d}z} C_{\mathrm{DFG}}^m + \frac{\alpha_3^m}{2} C_{\mathrm{DFG}}^m = \mathrm{i}\beta_{\mathrm{DFG}}^{ml'l''q} A_0^{q*} B_0^{l'} B_0^{l''} \times\exp\left(-\mathrm{i}\Delta k_{\mathrm{DFG}}^{ml'l''q} z - \frac{\alpha_1^q + \alpha_2^{l'} + \alpha_2^{l''}}{2}\,z\right). \qquad (50)$$

Here, the phase mismatch includes the dispersion of waveguide modes and can be represented as

$$\Delta k_{\mathrm{DFG}}^{ml'l''q} = K_3^m - K_2^{l'} - K_2^{l''} + K_1^q \approx \Delta k_{\mathrm{DFG}}^{\mathrm{g}} + \Delta k_{\mathrm{DFG}}^{\prime ml'l''q}\,, \qquad (51)$$

where

$$\Delta k_{\mathrm{DFG}}^{\mathrm{g}} = \frac{\omega}{c}\left[3n(3\omega) - 4n(2\omega) + n(\omega)\right], \qquad (52)$$

$$\Delta k_{\mathrm{DFG}}^{\prime ml'l''q} = \frac{c}{2\omega a^2}\left[\frac{(u^{l'})^2}{2} + \frac{(u^{l''})^2}{2} - \frac{(u^m)^2}{3} - (u^q)^2\right] \qquad (53)$$

are the components of the phase mismatch due to the dispersion of the gas and waveguide modes, respectively.

The nonlinear coefficient can be expressed in terms of the relevant nonlinear-optical cubic susceptibility [48]:

$$\beta_{\mathrm{DFG}}^{ml'l''q} = \frac{27\pi\omega^2}{K_3^m c^2}\,\chi_{\mathrm{DFG}}^{(3)}\,\frac{\iint f_3^m(\rho) f_2^{l'}(\rho) f_2^{l''}(\rho) f_1^q(\rho)\rho\,\mathrm{d}\rho\,\mathrm{d}\theta}{\iint\left[f_3^m(\rho)\right]^2\rho\,\mathrm{d}\rho\,\mathrm{d}\theta}\,, \tag{54}$$

where $\chi_{\mathrm{DFG}}^{(3)}$ is the third-order nonlinear-optical susceptibility responsible for difference-frequency generation.

Integrating Eqn (50), we derive the following expression for the amplitude of the DFG signal excited in the EH_{1m} mode:

$$C_{\mathrm{DFG}}^m = \mathrm{i}\beta_{\mathrm{DFG}}^{ml'l''q} A_0^{q*} B_0^{l'} B_0^{l''}\left\{\exp\left(-\frac{\alpha_3^m}{2}L\right) - \exp\left[\left(-\frac{\alpha_1^q+\alpha_2^{l'}+\alpha_2^{l''}}{2} - \mathrm{i}\Delta k_{\mathrm{DFG}}^{ml'l''q}\right)L\right]\right\} \times\left(\frac{\alpha_3^m-\alpha_1^q-\alpha_2^{l'}-\alpha_2^{l''}}{2} - \mathrm{i}\Delta k_{\mathrm{DFG}}^{ml'l''q}\right)^{-1}. \tag{55}$$

In the limiting case of low losses and zero phase mismatch, Eqn (55) can be reduced to

$$C_{\mathrm{DFG}}^m = \mathrm{i}\beta_{\mathrm{DFG}}^{ml'l''q} A_0^{q*} B_0^{l'} B_0^{l''} L\,. \tag{56}$$

Using Eqn (56), we derive the following estimate for the power of the DFG signal:

$$P_{\mathrm{DFG}} \sim P_1 P_2' P_2''\,\frac{L^2}{a^4}\,, \tag{57}$$

where P_2' and P_2'' are the powers of pump radiation at the frequency of the second harmonic in the relevant guided modes.

Expressions (49) and (57) describe the dependence of the FWM signal power on geometrical sizes of a hollow fiber. In Section 6.2.2, we will use these formulas to analyze the physical factors allowing the efficiency of four-wave mixing of short laser pulses to be increased in gas-filled hollow fibers.

6.2.2 Improving the efficiency of four-wave mixing in the waveguide regime. To illustrate how the efficiency of FWM processes can be improved by using hollow fibers, it would be instructive to consider the basic formulas of the elementary theory of four-wave mixing. Expressions for the powers of signals produced through FWM processes of third-harmonic and difference-frequency generation (generally, $\omega_{\mathrm{DFG}} = 2\omega_2 - \omega_1$) can be found in many textbooks on nonlinear optics (see, e.g., Refs [29, 30]). In particular, in the regime of loose focusing, when the condition

$$b \gg L \tag{58}$$

is satisfied, where b is the confocal parameter, these expressions can be written as

$$P_{\mathrm{THG}} \sim P_1^3\,\frac{L^2}{b^2}\,\frac{\sin^2\left[(\Delta k + 4/b)L/2\right]}{\left[(\Delta k + 4/b)L/2\right]^2} \tag{59}$$

in the case of third-harmonic generation,

$$P_{\mathrm{DFG}} \sim P_1 P_2^2\,\frac{L^2}{b^2}\,\frac{\sin^2(\Delta k L/2)}{(\Delta k L/2)^2}\,, \tag{60}$$

in the case of difference-frequency generation. Here, we used the following notation: P_1 and P_2 are the powers of the pump waves and Δk is the phase mismatch for the corresponding FWM process.

Let us consider in greater detail the enhancement of the efficiency of FWM processes in hollow fibers with respect to the geometry of tight focusing due to the increase in the interaction length of light beams attainable with hollow fibers. Physically, a hollow fiber enhances FWM processes since it allows light intensities typical of the tight-focusing regime to be achieved, simultaneously letting these beams interact in a nearly plane-wave regime.

Since the intensity of the FWM signal is proportional to the intensities of the pump beams, the power of the FWM signal can be increased by decreasing the diameter of a hollow fiber and keeping the powers of pump beams constant as long as the phase-matching conditions are satisfied and the losses of the waves interacting in the fiber are low. The role of a hollow fiber is thus to ensure the regime of interaction of collimated beams [cf. Eqns (59), (60) and (49), (57)] for light beams having intensities typical of the regime of tight focusing, simultaneously providing large interaction lengths for these beams and improving the phase matching.

Figure 8 displays the phase mismatch calculated with the use of Eqns (43)–(45) and (51)–(53) for THG and DFG processes involving different waveguide modes as a function of the inner radius of a hollow fiber filled with atmospheric-pressure air under normal conditions. As can be seen from these plots, the phase mismatch for the DFG process involving fundamental waveguide modes of pump and signal radiation can be completely compensated with an appropriate choice of the hollow-fiber inner radius. In the case of third-harmonic generation in the field of the fundamental mode of pump radiation, phase matching can be achieved only for higher order modes of the hollow fiber. Generally, the phase-matching problem under these conditions can be solved by adjusting the gas pressure, choosing optimal parameters of the hollow fiber, and excitation of appropriate waveguide modes [40–42].

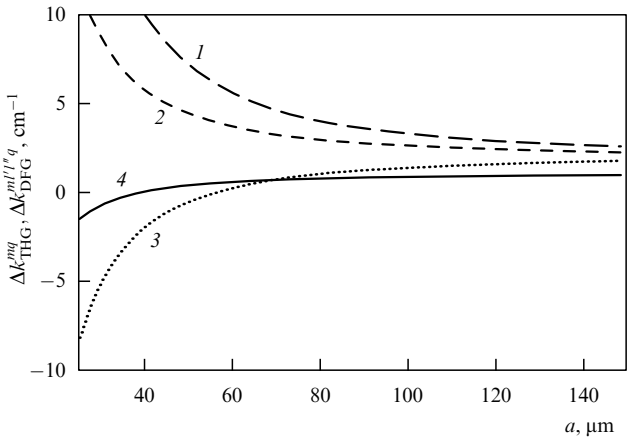

Figure 8. Phase mismatches for third-harmonic generation (*1–3*) and difference-frequency generation (*4*) in a hollow fiber filled with atmospheric-pressure air under normal conditions as functions of the inner radius of the fiber a. The transverse distribution of the pump field corresponds to the EH_{11} waveguide mode. The third harmonic is produced in the EH_{11} (*1*), EH_{12} (*2*), and EH_{13} (*3*) waveguide modes. The DFG signal is generated in the EH_{11} waveguide mode.

Thus, there are two natural ways of increasing the efficiency of nonlinear-optical processes in hollow fibers: (i) increasing the fiber length and (ii) reducing the inner radius of the fiber. The enhancement factor cannot be increased infinitely, of course. The increase of the fiber length is limited by optical losses of hollow-fiber modes, while the decrease of the inner radius requires a tighter focusing of the pump beam, eventually leading to the breakdown of the gas filling the fiber. The use of shorter pulses under these conditions allows a further improvement of the efficiency of nonlinear-optical processes due to the increase in the breakdown threshold of the gas.

6.2.3 Removing the prohibition on third-harmonic generation. Hollow fibers may play an even more important role in the case of sum-frequency and third-harmonic generation. In media with a normal dispersion, such FWM processes are characterized by a low efficiency in the tight-focusing regime due to an additional phase shift of a focused beam with respect to a plane wave. This geometric phase shift around the axis of a Gaussian beam can be written as [30]

$$\Delta\varphi = -\arctan\frac{2(z-z_0)}{b}\,, \tag{61}$$

where z_0 is the coordinate of the beam waist.

In accordance with Eqn (61), the phase shift between the field of the third harmonic and the nonlinear polarization responsible for THG tends to $\pm\pi$ as $z \to \pm\infty$. Therefore, no third harmonic can be observed at the output of the medium in this regime because of the destructive interference of the pump and third-harmonic fields generated before and after the focus.

The situation radically changes in the case of hollow fibers, where nonlinear-optical interactions occur in the regime of collimated light beams, giving rise to no $\pm\pi$ phase shift between the signal field and the relevant polarization of the medium. This allows efficient third-harmonic generation. Experimental results confirming this conclusion will be presented below.

6.3 Experimental setup

The experimental setup for studying FWM processes in gas-filled hollow fibers (Fig. 9) consisted of a picosecond laser system, which generated pump radiation at the wavelengths of 1.06 and 0.53 μm, a hollow fiber, and a detection system based on a photodetector, photomultiplier, and a CCD camera. The picosecond system included a passively mode-locked Nd:YAG master oscillator with negative-feedback-controlled cavity Q factor [71], a single-pulse selection unit, and amplifying stages. Passive mode locking in the master oscillator was implemented with the use of a saturable absorber film, which was placed in front of the rear cavity mirror and which made it possible to generate laser pulses with a duration of 35 ps.

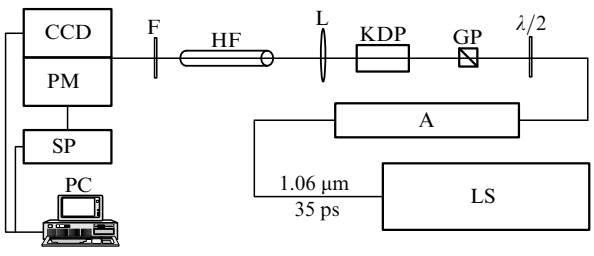

Figure 9. Diagram of the experimental setup for studying FWM processes in gas-filled hollow fibers based on a passively mode-locked picosecond laser system: LS, picosecond laser system; A, amplification stages; GP, Glan prism; L, achromatic lens; HF, hollow fiber; F, bandpass filter; PM, photomultiplier; CCD, CCD camera; SP, signal-processing unit; and PC, personal computer.

Negative feedback was introduced by inserting an electro-optical switch controlled with a fast-response photomultiplier inside the cavity. An optical signal served as the input for the fast-response photomultiplier. This feedback loop considerably improved the stability of parameters of laser pulses [74], providing an opportunity to generate trains of picosecond light pulses with a duration of the envelope on the order of 30 – 40 μs. As the regime of stationary lasing was established in the master oscillator, the negative feedback loop was switched off, and a short train of highly stable picosecond pulses with a duration of the envelope of about 100 ns and an energy of approximately 1.5 mJ was generated.

An electro-optical switch was used to separate a single pulse from this train. The energy of a single 35-ps laser pulse thus selected ranged from 30 to 40 μJ. The single-pulse selection unit also served as an optical decoupler, suppressing the parasitic feedback between amplifying stages and the master oscillator and preventing radiation reflected from optical elements of the amplification system from influencing the formation of trains of pulses in the master oscillator. Further details of this picosecond laser system can be found elsewhere [71, 74].

A single pulse of 1.06-μm radiation passes through three amplifying stages. The energy of the laser pulse at the output of the third stage may reach 50 mJ. The spatial distribution of intensity in such a laser beam is close to that characteristic of the Gaussian mode. This radiation was used as a pump beam in the THG scheme and one of the pump beams in sum- and difference-frequency generation. A KDP crystal was used to produce the second harmonic of Nd:YAG laser radiation for two-color experiments. A spherical lens was employed to couple pump beams into the fiber (see Fig. 9).

We used commercially available hollow fibers with inner diameters of 70, 100, 127, 152, and 203 μm in our experiments. The lengths of the fibers were varied from 1 up to 30 cm. The attenuation coefficients of 1.06-μm radiation in these fibers were estimated as 0.6, 0.2, 0.1, 0.06, and 0.04 dB cm^{-1}, respectively. The signals produced through third-harmonic, sum-frequency, and difference-frequency generation in these fibers were selected with a monochromator and bandpass filters and were detected with a photomultiplier. A CCD camera was used to investigate the spatial profiles of light beams coming out of the fiber.

Gas-pressure dependences of nonlinear-optical signals were measured with an experimental setup (Fig. 10) consisting of a picosecond laser, a vacuum chamber with a hollow fiber inside, and a detection system based on a photomultiplier. The Nd:YAG picosecond laser generated 50-ps pump pulses at 1.06 and 0.53 μm. The maximum energy of 1.06-μm radiation reached 100 mJ. A KDP crystal was used to produce the second harmonic of fundamental radiation.

An achromatic lens was used to couple the pump laser beams into a hollow fiber. Two photodiodes were used to monitor the energies of both of these laser beams transmitted through the fiber. The energies of fundamental radiation and the second harmonic in these experiments were equal to 1 and

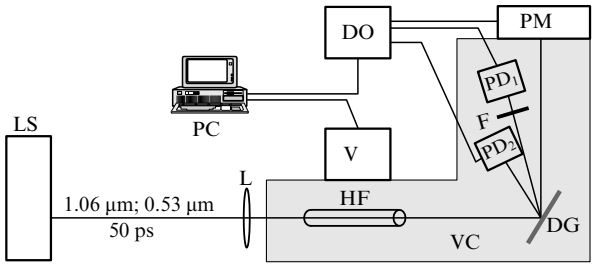

Figure 10. Diagram of the experimental setup for studying the influence of the gas pressure on FWM processes in a gas-filled hollow fiber: LS, picosecond laser system; L, achromatic lens; VC, vacuum chamber; HF, hollow fiber; DG, diffraction grating; PM, photomultiplier; F, filter blocking pump beams; PD_1 and PD_2, photodiodes measuring the energy of fundamental radiation and the second harmonic, respectively; DO, digital oscilloscope; V, computer-controlled valve for gas delivery.

0.1 mJ, respectively. The signal produced through an FWM process in a hollow fiber was detected with a photomultiplier and was then processed and displayed with a digital oscilloscope. The result of averaging over 30 FWM pulses was stored in a personal computer.

6.4 The influence of higher order waveguide modes

The results of our experiments [47, 48] fully justify our expectations that the use of hollow fibers allows the efficiency of FWM processes to be improved, the prohibition on THG to be removed, and phase-matching conditions in FWM processes to be improved. Our experiments also revealed a noticeable influence of higher order waveguide modes on FWM processes in gas-filled hollow fibers. The processes of four-wave mixing $3\omega = 2\omega + 2\omega - \omega$ involving different guided modes observed in experiments [47, 48] are presented in Table 1, where the transverse distributions of light field intensity in waveguide modes are also shown.

Table 1. Four-wave mixing $3\omega = 2\omega + 2\omega - \omega$ involving different guided modes of a gas-filled hollow fiber and transverse intensity distributions of the light field in these modes.

2ω	2ω	ω	3ω
EH_{11}	EH_{11}	EH_{11}	EH_{11}
EH_{11}	EH_{13}	EH_{12}	EH_{12}
EH_{11}	EH_{14}	EH_{13}	EH_{11}
EH_{11}	EH_{11}	EH_{11}	EH_{12}
EH_{11}	EH_{12}	EH_{11}	EH_{13}

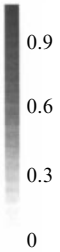

The power of the DFG signal at the frequency $\omega_{DFG} = 2\omega_2 - \omega_1$ (where ω_1 is the frequency of fundamental radiation of the Nd:YAG laser and $\omega_2 = 2\omega_1$ is the frequency of the second harmonic of this laser) is linear in the fundamental radiation power and quadratic in the power of the second harmonic of the Nd:YAG laser. These results indicate that nonlinear-optical interactions in our experiments occur in the weak-field regime, and effects related to the ionization of the medium and the self-action of pump pulses do not exert a considerable influence on nonlinear-optical processes. This conclusion is also supported by the fact that no THG signal was observed in our experiments in the tight-focusing regime with the same focusing parameters as in hollow-fiber experiments, but in the absence of a hollow fiber, until a plasma was produced due to the gas breakdown. The THG signal was easily detectable under conditions of ionization of the medium and ionization-induced self-action of pump pulses [57, 58].

The influence of phase-matching effects on FWM processes in hollow fibers is illustrated by the experimental data presented in Fig. 11. In particular, these experimental data indicate that, for gases whose dispersion properties are similar within the studied frequency range, the pressure dependences of the DFG signal power have much in common. Specifically, the pressure dependences of the DFG signal for argon and nitrogen display qualitatively similar tendencies.

At the same time, the pressure dependence of the DFG signal for carbon dioxide qualitatively differs from similar dependences for argon and nitrogen. This is due to considerable differences in the dispersion properties of carbon dioxide and those of argon and nitrogen. In particular, the phase mismatch for the DFG process at the atmospheric pressure of carbon dioxide is estimated as $\Delta k^{g}_{DFG} = 1.8\ cm^{-1}$, which noticeably differs from the phase mismatch corresponding to the atmospheric pressure of nitrogen or argon ($\Delta k^{g}_{DFG} = 1\ cm^{-1}$).

Comparison of the experimental data presented in Figs 12–14 with the results of calculations performed with the use of Eqns (51)–(53) and (55) reveals a noticeable role of higher order waveguide modes in nonlinear-optical processes in hollow fibers. It is instructive in this context to consider in greater detail the results obtained for the DFG process $\omega_{DFG} = 2\omega_2 - \omega_1$ $(3\omega = 2\omega + 2\omega - \omega)$ in an argon-filled hollow fiber with a length of 17.4 cm and an inner diameter $a = 100$ μm.

A satisfactory agreement between the experimental data (squares) and theoretical predictions (the solid lines) is achieved when effects related to higher order waveguide modes are included in the analysis. In particular, a satisfactory agreement between the experimental data in Fig. 12 and the results of calculations performed with the use of Eqns (51)–(53) and (55) was achieved when not only the DFG process occurring in the fundamental waveguide mode (i.e., the DFG process involving the EH_{11} hollow-fiber modes of fundamental radiation, second harmonic, and the DFG signal; the first line of Table 1), but also the DFG process involving the EH_{12} mode of fundamental radiation, EH_{11} and EH_{13} modes of the second harmonic, and the EH_{12} mode of the DFG signal (the second line of Table 1) was included in calculations.

The maximum of the DFG signal around an argon pressure of about 0.7 atm is observed within the pressure range where the DFG process in the fundamental waveguide

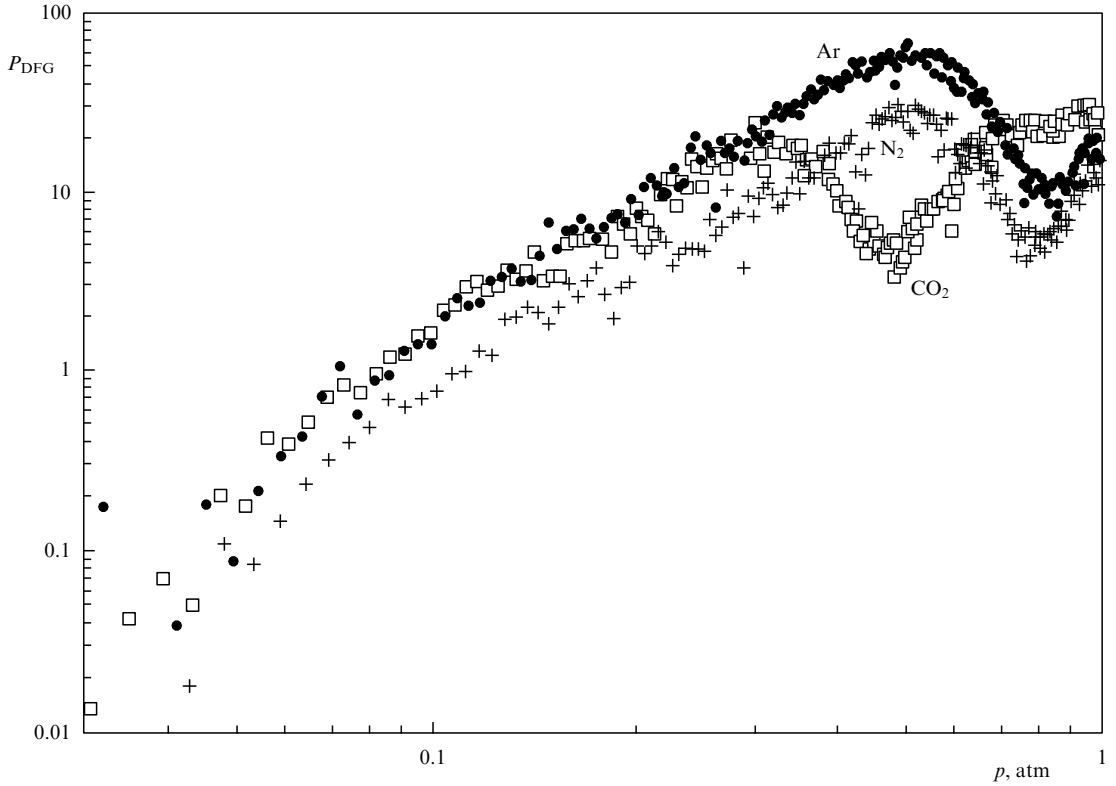

Figure 11. Power of the difference-frequency signal produced in a hollow fiber filled with different gases (Ar, N_2, and CO_2) as a function of the gas pressure p. The fiber length is 19.3 cm. The inner diameter of the fiber is 127 μm.

mode is phase-matched (the dashed line in Fig. 12 shows the phase mismatch for this process). At lower pressures, difference-frequency generation through the FWM interaction of the EH_{12} mode of fundamental radiation, EH_{11} and EH_{13} modes of the second harmonic, and the EH_{12} mode of the DFG signal begins to play a more important role (the phase mismatch for this process is shown by the dash-dotted line in Fig. 12). Thus, higher order waveguide modes of a hollow fiber may have a noticeable influence on FWM processes.

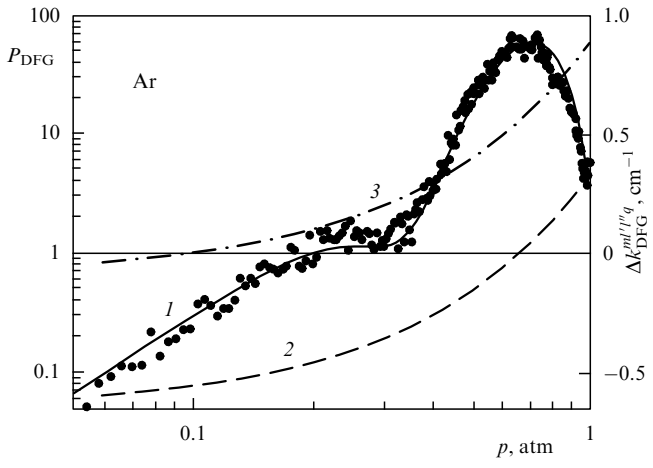

Figure 12. Power of the difference-frequency signal (the dots show the experimental data, and solid line *1* represents the results of calculations) and the phase mismatch for the DFG process in an argon-filled hollow fiber as functions of the argon pressure p. The dashed line *2* shows the phase mismatch for the DFG process occurring in the fundamental waveguide mode EH_{11}. The dash-dotted line *3* represents the phase mismatch for the DFG process involving the EH_{12} mode of fundamental radiation, EH_{11} and EH_{13} modes of the second harmonic, and the EH_{12} mode of the DFG signal. The length of the hollow fiber is 17.4 cm, and the inner diameter is 100 μm.

The results of our experiments also show that the role of higher order waveguide modes in nonlinear-optical processes in a hollow fiber becomes more significant with increasing inner diameter of the fiber. Figure 13 presents the results of experiments performed for the FWM process $3\omega = 2\omega + 2\omega - \omega$ in an argon-filled hollow fiber with a length of 20.1 cm and an inner diameter 203 μm. To achieve a reasonable agreement between the experimental data (the dots) and the results of calculations (solid line *1*) in this case, we have to take into consideration FWM processes involving the EH_{11} and EH_{13} waveguide modes of fundamental radiation, the EH_{11}, EH_{12}, and EH_{14} waveguide modes of the second harmonic, and the EH_{11}, EH_{12}, and EH_{13} modes of the FWM signal (the phase mismatches for these FWM processes are shown by dashed lines *2* – *5* in Fig. 13).

The maximum of the FWM signal observed around an argon pressure of 0.25 atm then corresponds to the phase matching of the FWM process in the fundamental waveguide mode (the first line of Table 1; the phase mismatch for this process is shown by dashed line *2* in Fig. 13). For an argon pressure of 0.6 atm, the chosen length of the fiber is close to a tripled coherence length of the considered FWM process ($L = 3L_{coh}$).

The maximum of the FWM signal observed around an argon pressure of 0.9 atm corresponds to the phase matching of the FWM process involving the EH_{11} modes of fundamental radiation and the second harmonic and the EH_{12} mode of the FWM signal (the fourth line of Table 1; the phase mismatch for this process is shown by the dashed line *4* in

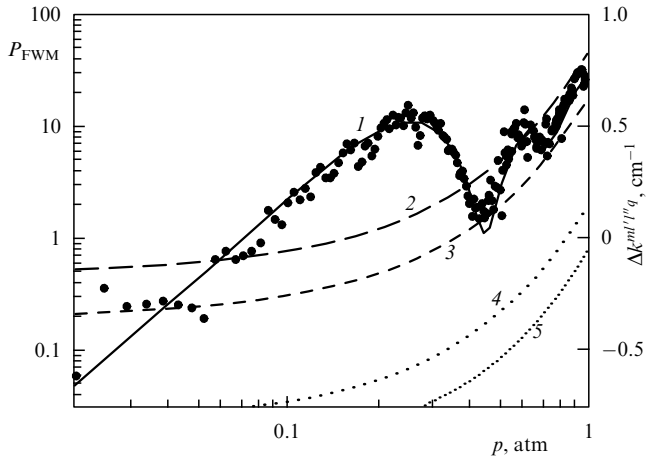

Figure 13. Power of the FWM signal (the dots show the experimental data, solid line *1* represents the results of calculations) and the phase mismatch for the FWM process in an argon-filled hollow fiber as functions of the argon pressure p. The dashed line *2* shows the phase mismatch for the FWM process occurring in the fundamental waveguide mode EH_{11}. The dashed and dotted lines *3*–*5* represent the phase mismatches for FWM processes involving (*3*) the EH_{13} mode of fundamental radiation, the EH_{11} and EH_{14} modes of the second harmonic, and the EH_{11} mode of the FWM signal; (*4*) the EH_{11} modes of fundamental radiation and the second harmonic and the EH_{12} mode of the FWM signal; and (*5*) the EH_{11} mode of fundamental radiation, the EH_{11} and EH_{12} modes of the second harmonic, and the EH_{13} mode of the FWM signal. The length of the hollow fiber is 20.1 cm, and the inner diameter is 203 μm.

Fig. 13), as well as the FWM process involving the EH_{11} mode of fundamental radiation, the EH_{11} and EH_{12} modes of the second harmonic, and the EH_{13} mode of the FWM signal (the fifth line of Table 1; the phase mismatch for this process is shown by the dashed line *5* in Fig. 13).

The four-wave mixing of the EH_{13} mode of fundamental radiation, the EH_{11} and EH_{14} modes of the second harmonic, and the EH_{11} mode of the FWM signal (the third line of Table 1) provides a noticeable contribution to the total FWM signal within the range of argon pressures from 0.3 up to 0.4 atm, where this FWM process is phase-matched (the dashed line *3* in Fig. 13).

Figure 14 displays the power of the DFG signal generated in argon-filled hollow fibers with different inner diameters and a length of $\sim$ 20 cm as a function of the argon pressure p. As can be seen from Fig. 14, the maximum of the DFG signal related to the all-fundamental-mode FWM process is shifted toward lower pressures with an increase in the inner diameter of the hollow fiber, approaching its limiting position corresponding to the FWM process in collimated beams. In this limiting case, the maximum power of the DFG signal is achieved, in accordance with Eqn (37), for a gas pressure in the fiber equal to 0.16 atm (at this pressure, the coherence length of the DFG process, $L_{ph} = \pi/\Delta k^{g}_{DFG}$, becomes equal to the fiber length).

Thus, the results of these measurements agree well with our expectations based on the analysis of Eqns (28) – (30). The maxima observed in the DFG signal at an argon pressure of about 0.7 atm for a hollow fiber with an inner diameter of 152 μm and a pressure of 0.9 atm for a fiber with an inner diameter of 203 μm can be attributed, by analogy with the case considered above, to FWM processes involving higher order waveguide modes of the pump and FWM beams.

Thus, the results of experimental and theoretical studies presented above reveal several important features of nonlinear-optical processes in gas-filled hollow fibers, giving a deeper insight into methodological aspects of the problem and opening new possibilities for practical applications of hollow fibers in nonlinear optics, the optics of ultrashort

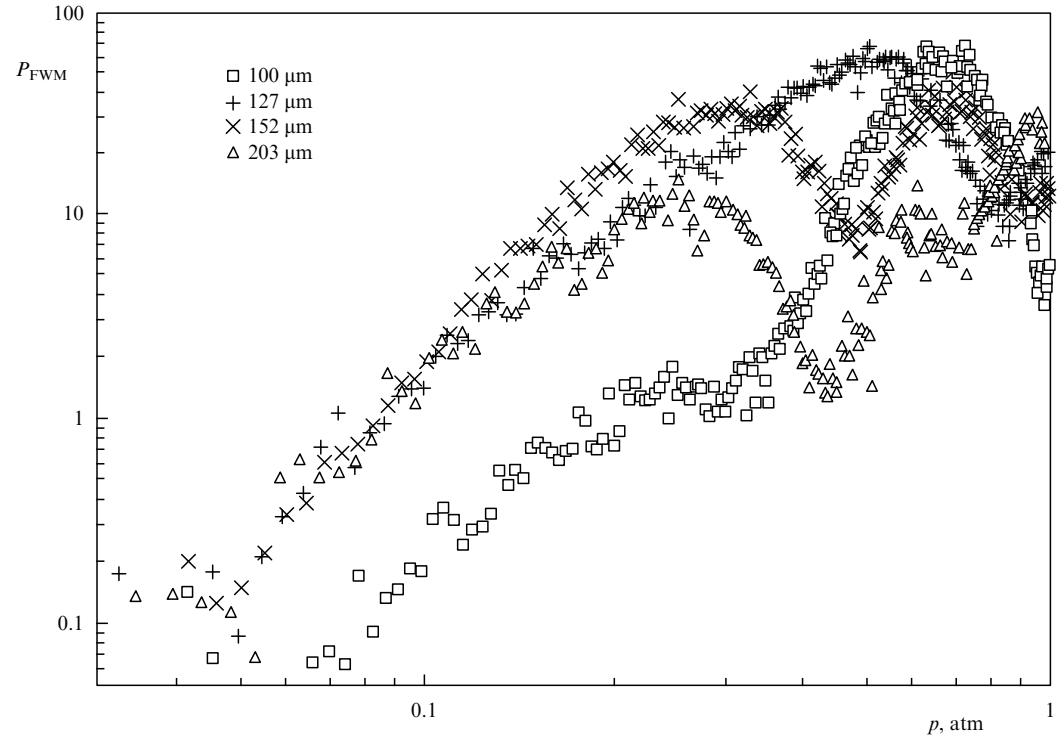

Figure 14. Power of the FWM signal in argon-filled hollow fibers with different inner diameters as a function of the argon pressure p. The length of hollow fibers in all the experiments was approximately equal to 20 cm.

pulses, and nonlinear spectroscopy. Due to the improvement of phase-matching conditions with an appropriate choice of the gas pressure and optimal parameters of the hollow fiber, we were able to use hollow fibers with a large length (up to 30 cm) for difference-frequency generation, which resulted in a considerable increase in the power of the difference-frequency signal at the output of the fiber.

Our experimental results indicate that higher order waveguide modes may have a considerable influence on four-wave mixing processes in gas-filled hollow fibers. This effect can be employed to increase the total energy of short-wavelength radiation produced through nonlinear-optical processes in hollow fibers. On the other hand, effects related to higher order waveguide modes should be taken into consideration in the optimization of hollow-fiber frequency converters and pulse compressors, where the excitation of higher order waveguide modes may lead to unwanted energy losses.

Finally, the experiments discussed above have shown that the waveguide regime of nonlinear-optical interactions implemented in hollow fibers removes the limitations on the efficiency of third-harmonic and sum-frequency generation, which are characteristic of the tight-focusing regime in media with normal dispersion and which are due to the geometric phase shift arising in tightly focused light beams. This finding suggests that hollow fibers can considerably expand the possibilities of frequency conversion and nonlinear-optical spectroscopic gas-phase analysis.

7. High-order harmonic generation in gas-filled hollow fibers

7.1 Hollow fibers as sources of coherent short-wavelength radiation

High-order harmonic generation in hollow fibers suggests promising ways for producing few-cycle pulses with simultaneous frequency conversion of laser radiation. The improvement of the efficiency of high-order harmonic generation and the control of the temporal and spatial phase distribution in optical harmonics are currently the key issues in the synthesis of ultrashort pulses (including subfemtosecond pulses) with controlled parameters.

Hollow fibers allow the length of nonlinear-optical interactions to be radically increased and phase and group-velocity matching to be achieved, thus offering new possibilities for improving the efficiency of high-order harmonic generation. The results of experimental studies [43 – 46] have demonstrated that, due to the compensation of phase mismatch in hollow fibers, the efficiency of frequency conversion in high-order harmonic generation can be increased by a factor of 100 – 1000 as compared with the efficiencies of frequency conversion attainable in experiments with gas jets. A conversion efficiency of 4×10^{-5} has been achieved by Constant et al. [45] for the 15th harmonic generated in a hollow fiber filled with xenon with the use of 40-fs 1.5-mJ 800-nm pulses.

Figure 15 illustrates the possibility of increasing the efficiency of high-order harmonic generation due to improved phase matching. This figure presents the results of calculations [61] for the enhancement η of generation of high-order harmonics of 790-nm fundamental radiation in a 150-μm-inner-diameter hollow fiber filled with different rare gases (helium, neon, and argon). The transverse distribution of the pump intensity was assumed to correspond to the EH_{11} waveguide mode.

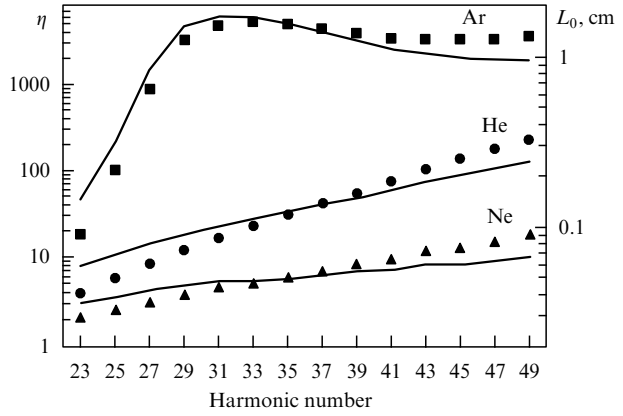

Figure 15. Enhancement η of high-order harmonic generation due to waveguide phase matching (points) and the absorption length $L_0 = 1/2\varkappa_q$ corresponding to the optimal gas pressure p_0 allowing the harmonic-generation process to be phase-matched (solid lines) in a 150-μm-inner-diameter hollow fiber filled with different rare gases (helium, neon, and argon) in the absence of ionization. The wavelength of pump radiation is 790 nm. The transverse distribution of the pump intensity corresponds to the EH_{11} waveguide mode.

The phase of high-order harmonics can be controlled by choosing the initial chirp of the pump pulse [75], by varying the position of the pump-beam waist relative to the nonlinear medium [76], by applying a biharmonic pump [77, 78], and by preparing the initial state of a harmonic-generating system in the form of a coherent superposition of quantum states [79]. In particular, by applying a linearly chirped pump field to compensate for the phase of the nonlinear polarization induced in a medium by the laser field, one can efficiently control the shape of the spectrum of high-order harmonics [75] and to compress pulses of optical harmonics through the compensation of their chirp [80].

7.2 The nonlinear-optical response and propagation effects

Analysis of harmonic generation in hollow fibers includes two stages: (i) calculation of the nonlinear-optical response of an atomic, ionic, or molecular system responsible for high-order harmonic generation [68, 69, 81 – 86] and (ii) solution of the wave equation governing the relevant propagation effects [85 – 87]. Many important physical aspects related to the nonlinear-optical response of a gas medium can be understood in terms of the quasiclassical model of harmonic generation developed in Refs [82, 83].

The quantum-mechanical analysis of the nonlinear-optical response [84 – 86] gives the following expression for the complex amplitude of the qth harmonic:

$$d_q \propto \sum_s \frac{\exp\left[-\mathrm{i}S(\mathbf{p}_s, t_s, \tau_s) + \mathrm{i}qt_s\right]}{(\mathrm{i}\tau_s/2 + \varepsilon)^{3/2}\left[\det(t_s, \tau_s)\right]^{1/2}}, \tag{62}$$

where

$$S(\mathbf{p}, t, t') = \int_{t'}^{t} \left\{ \frac{1}{2}\left[\mathbf{p} - \mathbf{A}(t'')\right]^2 + I_\mathrm{p} \right\} \mathrm{d}t'' \tag{63}$$

is the quasiclassical action; $\mathbf{p} = \mathbf{v} + \mathbf{A}(t)$ is the canonic momentum; $\det(t_s, \tau_s)$ is the determinant of a 2×2 matrix involving second-order derivatives of the action in t_s and τ_s;

ε is a small positive quantity; and I_p is the ionization potential [Eqns (62) and (63) are written using the atomic system of units]. The summation in Eqn (62) is performed over the saddle points, which can be found from a set of equations [84–86] expressing the condition that an electron moving along a certain trajectory returns to its parent ion after the time interval τ_s, the energy-conservation law, and the equation governing the tunneling of an electron at the moment of time $t_s - \tau_s$.

As shown in Refs [84–86], within the range of frequencies above the cut-off frequency, the amplitude and the phase of harmonics are mainly determined by a single type of trajectory of electrons returning to a parent ion with the energy corresponding to the emitted harmonic. Analysis of Eqn (62) can be then restricted to a single term corresponding to the solution of the considered equations for saddle points that provide a dominant contribution to the process of harmonic generation. The phase of harmonics in this case is determined by the classical action corresponding to this saddle point.

The situation becomes much more complicated within the plateau region of the harmonic spectrum, where the approximation of a single stationary point is no longer sufficient [84–86] and at least two types of quasiclassical trajectories should be taken into consideration. Each of these types of trajectory is characterized by its own phase, which depends on the pump field intensity, resulting in complicated interference effects [85].

Propagation effects may have a considerable influence on the phase of the field of optical harmonics. In particular, propagation effects, as shown in [88, 89], may filter under certain conditions the contribution of one type of electron trajectory, allowing the formation of ultrashort pulses. Ionization effects give rise to a dynamic phase shift of the harmonic field [60, 61, 90], considerably changing phase matching and the efficiency of high-order harmonic generation. Such effects are briefly discussed in the following section.

7.3 Ionization effects

A straightforward way to improve the efficiency of nonlinear-optical interactions underlying pulse-compression and frequency-conversion applications of hollow fibers is to increase the intensity of laser pulses coupled into a fiber. Although the breakdown threshold for gas-filled fibers is much higher than the breakdown threshold for ordinary fibers, it would be natural to expect that the influence of ionization effects on the dispersion of a gas-filled fiber and nonlinear-optical processes in such a fiber should increase with the growth in the laser field coupled into the fiber.

Suppose that the light fields are sufficiently weak to allow a perturbative analysis of nonlinear-optical interactions in a hollow fiber. Then, in the regime where the slowly varying envelope approximation is applicable, pump depletion is negligible, and the number of atoms undergoing ionization is small, the intensity of the qth-order harmonic generated in a hollow fiber filled with a nonlinear gas undergoing weak pump-induced ionization is governed by the following expression [60, 61]:

$$I_q(\theta, \mathbf{\rho}) = 2\pi K_q q\omega \left| P_q^{\mathrm{NL}}(\theta, \mathbf{\rho}) \right|^2 \times \left| \frac{1 - \exp\left[-\mathrm{i}\Delta k_q^n(\theta) z - \varkappa_q z\right]}{-\mathrm{i}\Delta k_q^n(\theta) - \varkappa_q} \right|^2, \quad (64)$$

where $\theta = t - z/v$; v is the group velocity of the pump and harmonic pulses; K_q is the waveguide propagation constant of the harmonic pulse; ω is the pump frequency; $P_q^{\mathrm{NL}}(\theta, \mathbf{\rho})$ is the amplitude of the nonlinear polarization induced in the gas at the frequency of the harmonic; $2\varkappa_q$ is the absorption coefficient of qth-harmonic radiation; and

$$\Delta k_q^n(\theta) \approx \Delta k_0 + \Delta k_{\mathrm{w}}^n + \delta k_q^n(\theta) \quad (65)$$

is the phase mismatch including the phase mismatch due to waveguide dispersion, with

$$\Delta k_0 = \frac{q\omega}{c}\left[n_1(q\omega) - n_1(\omega)\right], \quad \Delta k_{\mathrm{w}}^n, \quad \text{and} \quad \delta k_q^n(\theta)$$

being the components of the phase mismatch related to gas dispersion, waveguide modes, and electrons emerging from ionization.

The inclusion of ionization effects in the analysis of pulse propagation and harmonic generation in hollow fibers generally requires the use of some model of ionization allowing the calculation of the ionization rate $w(I)$. In Refs [60, 90], the influence of ionization effects on high-order harmonic generation in hollow fibers was analyzed with an assumption of rectangular laser pulses. A rectangular pulse gives rise to a linear growth in the effective electron concentration as a function of time (see the inset in Fig. 16). Although grossly oversimplified, such an approach, however, reveals some important features of the influence of ionization on phase matching in harmonic generation in hollow fibers without specifying the ionization model.

Figure 17 shows the energy of the 27th harmonic pulse

$$E_q = \iiint I_q(\theta, \mathbf{\rho})\, \mathrm{d}\mathbf{\rho}\, \mathrm{d}\theta$$

(q is the harmonic number) as a function of the gas pressure in an argon-filled hollow fiber with an inner diameter of 150 μm in the absence of ionization (dashed line *1*) and when 0.8% of

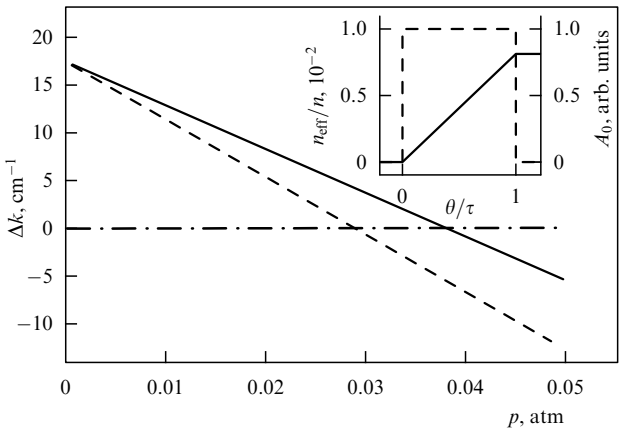

Figure 16. Phase mismatch for the 27th harmonic of 790-nm fundamental radiation generated in an argon-filled hollow fiber with an inner diameter of 150 μm as a function of the gas pressure on the leading edge of the pulse (dashed line), where ionization does not play an important role, and on the trailing edge of the pulse (solid line), where 0.8% of atoms are ionized. The transverse distribution of the pump intensity corresponds to the EH_{11} waveguide mode. The pump pulse has a rectangular shape (the dashed line in the inset), giving rise to a linear growth in the effective electron concentration as a function of time θ (the solid line in the inset).

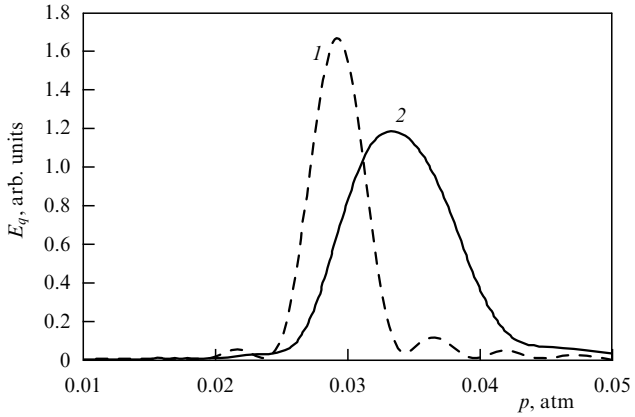

Figure 17. Energy of the 27th harmonic of 790-nm fundamental radiation generated in an argon-filled hollow fiber with an inner diameter of 150 μm as a function of the gas pressure in the absence of ionization (dashed line *1*) and when 0.8% of atoms are ionized during the pump pulse (solid line *2*). The transverse distribution of the pump intensity corresponds to the EH_{11} waveguide mode. The pump pulse is assumed to have a rectangular shape (see the inset in Fig. 16).

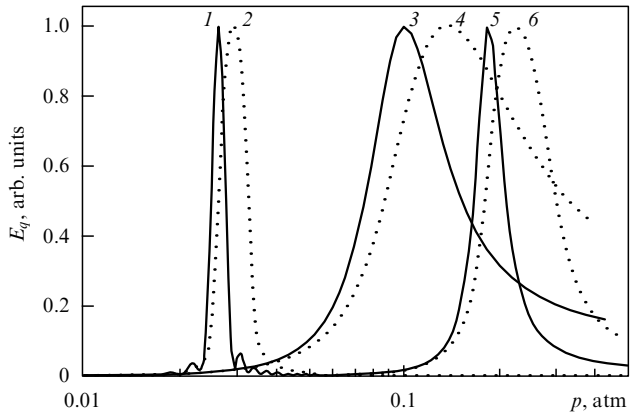

Figure 18. Energy of the 41st harmonic of 790-nm fundamental radiation generated in a 150-μm-inner-diameter 2-cm-long hollow fiber filled with argon (curves *1*, *2*), neon (curves *3*, *4*), and helium (curves *5*, *6*) calculated as a function of the gas pressure in the absence of ionization (solid lines *1*, *3*, *5*) and in the regime of ionization governed by the ADK formula (dotted lines *2*, *4*, *6*). The transverse distribution of pump intensity corresponds to the EH_{11} waveguide mode. The energy of a 70-fs rectangular pump pulse was set equal to 0.65 mJ (*2*), 1.75 mJ (*4*), and 2.3 mJ (*6*).

atoms are ionized during the pump pulse (solid line *2*) in the case when the transverse distribution of the pump intensity corresponds to the EH_{11} waveguide mode and the pump pulse has a rectangular shape (see the inset in Fig. 16). As can be seen from Fig. 17, the ionization of only 0.8% of argon atoms significantly changes the pressure dependence of the harmonic energy. Since the gas filling the fiber now undergoes ionization during the pump pulse, the contribution of free electrons to the refractive index of the gas leads to the phase modulation of the pump pulse.

Due to the change in the phase of the pump pulse from its leading edge to the trailing edge, the phase mismatch for harmonic generation changes within the pump pulse. Figure 16 shows the phase mismatch for the 27th harmonic of 790-nm fundamental radiation generated in an argon-filled hollow fiber with an inner diameter of 150 μm calculated [60] as a function of the gas pressure (the dashed line) on the leading edge of the pulse, where ionization does not play an important role, and (the solid line) on the trailing edge of the pulse, where 0.8% of atoms are ionized. It was assumed in those calculations that the transverse distribution of pump intensity corresponds to the EH_{11} waveguide mode. The pump pulse has a rectangular shape (the dashed line in the inset), giving rise to a linear growth in the effective electron concentration as a function of time θ (the solid line in the inset). As can be seen from Fig. 16, the phase mismatch in an ionizing gas is a function of time θ. Therefore, different pressures would be required to phase-match harmonic generation at different θ (see Fig. 16). The net effect of ionization occurring in the gas filling the fiber is that it decreases the overall efficiency of harmonic generation and makes the harmonic-generation efficiency less sensitive to the gas pressure in the hollow fiber.

Figure 18 shows the energy of the 41st harmonic of 790-nm fundamental radiation generated in a 150-μm-inner-diameter 2-cm-long hollow fiber filled with argon (curves *1*, *2*), neon (curves *3*, *4*), and helium (curves *5*, *6*) calculated [61] as a function of the gas pressure. The ionization probability was calculated in accordance with the Ammosov – Delone – Kraĭnov (ADK) formula [91]. Ionization processes (dotted curves *2*, *4*, *6*) shift the maxima in the dependences of the harmonic energy on the gas pressure in the fiber relative to the positions of these maxima in the absence of ionization (solid lines *1*, *3*, *5*).

Thus, we have shown that a weak ionization of the gas filling the fiber during the pump pulse gives rise to an electronic contribution to the refractive index of the gas and, consequently, to the phase modulation of the pump pulse. Due to this change in the phase of the pump pulse from its leading edge to the trailing edge, the phase mismatch for harmonic generation changes within the pump pulse, decreasing the overall efficiency of harmonic generation, but making the harmonic-generation efficiency less sensitive to the gas pressure in the hollow fiber.

8. Synthesis of ultrashort light pulses in a hollow fiber with a Raman-active gas

8.1 Nonlinear-optical processes in gas media and horizons of attosecond optics

One of the most promising and exciting directions of studies currently performed with gas-filled hollow fibers involves the synthesis of ultrashort laser pulses through high-order stimulated Raman scattering [11, 13 – 16, 92 – 94]. According to the theoretical analysis carried out in Refs [13 – 16, 92 – 94], such an approach may allow the generation of subfemtosecond and attosecond pulses.

Generation of extremely short light pulses, including pulses in the subfemtosecond range of durations, is one of the key issues in modern physics. Several possibilities for generating subfemtosecond and attosecond pulses are currently being discussed. One of the ways that leads beyond the femtosecond range is based on high-order harmonic generation in gas jets [31 – 35] and plasmas created on the surface of a solid target [36]. The spectrum of harmonics produced in an intense laser field features a plateau with approximately equal harmonic amplitudes. As shown in Refs [88, 89, 95 – 97], sequences of attosecond pulses can be synthesized by phase-locking these high-order harmonics (similar ideas have been discussed earlier in Refs [98, 99]).

The ways to solve the phase-locking problem are now being extensively discussed in the literature [88, 89, 95–97]. The methods of selection of single pulses out of pulse trains synthesized under such conditions are also being explored [95, 96]. Christov et al. [100] have pointed out the possibility of producing single attosecond pulses through harmonic generation in a gas in the field of ultrashort laser pulses (with durations on the order of 5 fs). Theoretical predictions concerning the possibility of synthesizing trains of attosecond pulses from phase-locked optical harmonics have been confirmed recently by the results of experiments [12], demonstrating that a group of high-order harmonics can be emitted under certain conditions in the form of a sequence of 250-as pulses.

Another direction in ultrashort-pulse generation involves the studies of high-order stimulated Raman scattering and the methods of phase-locking Stokes and anti-Stokes sidebands produced in Raman-active media [11, 13–16, 92–94]. These studies have shown, in particular, that superintense laser fields are, in fact, not necessary for the generation of attosecond pulses. Stokes and anti-Stokes sidebands can be produced with high efficiencies even in pump fields of moderate intensities, and phase relations suitable for synthesizing subfemtosecond and attosecond pulses can be provided for these sidebands with an appropriate excitation of Raman modes. As demonstrated by recent experiments [11], this approach allows the generation of pulses as short as 3.8 fs.

In this section, we will discuss in greater detail the possibilities of ultrashort-pulse synthesis through the generation of multiple Stokes and anti-Stokes sidebands in a Raman-active medium pre-excited with a short laser pulse. This method of short-pulse generation has been proposed and experimentally implemented in Refs [11, 13–16]. The main idea of this approach can be described in the following way. A short laser pulse with a duration less than the vibration cycle of a Raman-active vibration in a medium is used to pre-excite such vibrations of gas molecules. The molecular vibrations thus excited then modulate a probe pulse, which enters the medium with some delay time relative to the pump pulse. Amplitude and phase relations between multiple Stokes and anti-Stokes sidebands arising as a result of this process are suitable for synthesizing extremely short light pulses.

Important advantages of this approach to short-pulse generation are due to the fact that the preparation of a medium with a high-power laser pulse in this case is separated in time from the generation of Stokes and anti-Stokes sidebands in the field of a probe pulse with a moderate intensity. Numerous competing processes, having a detrimental effect on the formation of short pulses, such as self-action of laser pulses, ionization of a medium, and broadening and shifting of Stokes and anti-Stokes sidebands, can be eliminated under these conditions.

A hollow fiber with a length of 70–100 cm was used in experiments [14–16] to increase the length of interaction of pump and probe pulses with a Raman-active gas. With such interaction lengths, the group delay of the pump and probe pulses may become one of the important factors limiting the duration of pulses synthesized with the use of this technique. We will show below that a hollow fiber may serve not only to increase the interaction length, but also to reduce the influence of group-delay effects in such experiments. The group-velocity mismatch of the pump and probe pulses can be considerably decreased in a hollow fiber with an appropriate choice of the gas pressure, the inner diameter of the hollow fiber, and waveguide modes involved in the wave-mixing process. This allows the number of Stokes and anti-Stokes sidebands to be considerably increased by using longer hollow fibers, thus providing an opportunity to substantially reduce the duration of light pulses synthesized with the use of this approach.

8.2 The influence of group-delay effects on the synthesis of ultrashort light pulses

We will analyze the possibilities of synthesizing ultrashort pulses through the generation of multiple Stokes and anti-Stokes sidebands using the slowly varying envelope approximation. Although such an approximation is, rigorously speaking, inapplicable for a detailed description of the evolution of ultrashort light pulses, it permits some general tendencies in the evolution of the pulse and its spectrum to be understood. We will use this approximation to examine the role of group-delay effects in the synthesis of ultrashort light pulses in Raman-active gases and to illustrate the ways of reducing the group delay due to the waveguide dispersion.

Restricting our analysis to the case of EH_{1q} modes of a hollow fiber, we represent the fields of the pump and probe pulses propagating in a hollow fiber (Fig. 19) in the following form:

$$E_1 = \frac{1}{2} f^m(\rho)\, A(t,z) \exp\left[-\mathrm{i}(\omega_1 t - K_1^m z)\right] + \text{c.c.}\,, \qquad (66)$$

$$E_2 = \frac{1}{2} f^n(\rho)\, B(t,z) \exp\left[-\mathrm{i}(\omega_2 t - K_2^n z)\right] + \text{c.c.}\,, \qquad (67)$$

where ω_1 and ω_2 are the central frequencies of the pump and probe pulses, respectively; $f^q(\rho)$ is the transverse field distribution in the EH_{1q} mode of the hollow fiber; ρ is the distance from the axis of the hollow fiber; K_1^m and K_2^n are the propagation constants of the pump and probe pulses corresponding to the waveguide modes of the hollow fiber; and $A(t,z)$ and $B(t,z)$ are the slowly varying envelopes of the pump and probe pulses, respectively.

When the pump pulse (66) is switched off, Raman-active Q modes excited in the medium by this pulse freely decay in accordance with the following expression [15]:

$$Q(t) = Q_0 \exp\left(-\frac{t}{T_2}\right) \sin\left[\left(\Omega^2 - \frac{1}{T_2^2}\right)^{1/2} t\right], \qquad (68)$$

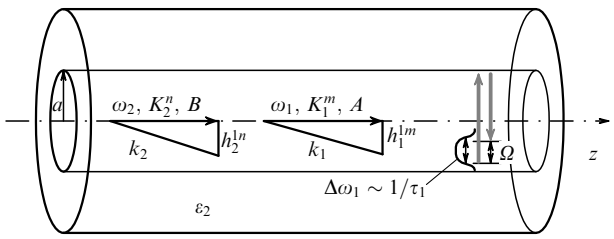

Figure 19. Propagation of light pulses in a gas-filled hollow fiber. The first pulse is used to excite Raman-active vibrations of molecules in the gas filling the fiber. The second pulse generates multiple Stokes and anti-Stokes sidebands in accordance with the approach developed in Refs [21–24]. The waveguide dispersion component compensates for the group-velocity mismatch of the pump and probe pulses; n_1 is the refractive index of the gas; ε_2 is the dielectric constant of the fiber cladding; h_1^{1m} and h_2^{1n} are the transverse wave numbers of guided modes.

where Q_0 is the amplitude of vibrations, which is proportional to the energy of the pump pulse; T_2 is the dephasing time of molecular vibrations; and Ω is the frequency of Raman-active vibrations.

The solution to the equation governing the evolution of the complex envelope of the probe pulse entering the Raman-active medium with some delay with respect to the pump pulse in the plane-wave regime under conditions when the dephasing time T_2 substantially exceeds the period of Raman vibrations and the durations of the light pulses has been found by Nazarkin et al. [15]. In the considered case of Raman scattering occurring in waveguide modes of a hollow fiber, the solution is formally given by the expression derived in Ref. [15],

$$B(\tau, z) = B(\tau, 0) \exp\left[-\mathrm{i}\gamma \frac{\sin(\Delta K_{mn} z)}{\Delta K_{mn}} \sin(\Omega\tau + \Delta K_{mn} z)\right], \tag{69}$$

where $\tau = t - z/v_2^n$, $B(\tau, 0)$ is the envelope of the input probe pulse,

$$\Delta K_{mn} = \frac{\Omega}{2}\left(\frac{1}{v_2^n} - \frac{1}{v_1^m}\right) \tag{70}$$

is the parameter characterizing the mismatch of the group velocities,

$$\gamma = \frac{2\pi}{c}\,\omega_2 N Q_0 \frac{\partial\alpha}{\partial Q}, \tag{71}$$

N is the concentration of Raman-active molecules in the gas, and $\partial\alpha/\partial Q$ is the derivative of the molecular polarizability in the vibrational coordinate. Expression (69) includes waveguide effects through the group velocities of light pulses, which are now defined in terms of the relevant propagation constants, and the coefficient γ, which is normalized in such a way as to include the transverse distributions of light fields in waveguide modes.

The spectrum of the probe pulse can now be represented as a superposition of equidistant spectral components $\omega_s = \omega_2 + s\Omega$ $(s = 0, \pm1, \pm2, \ldots)$, which are separated from each other by the frequency of molecular vibrations Ω. The number of Stokes and anti-Stokes sidebands in the spectrum of the probe pulse propagating in such an impulsively pre-excited Raman-active gas increases with the growth in the propagation length (Fig. 20). Under these conditions, the mismatch of the group velocities of the pump and probe pulses (the dashed lines in Fig. 21a, b) may be a serious problem for many gases, restricting the interaction length to the characteristic walk-off length $l_{mn}^{\mathrm{g}} = \pi/2\Delta K_{mn}$ which can be understood as the length where the group delay of the pump and probe pulses becomes equal to half the period of molecular Raman-active vibrations.

In particular, for pulses of 800- and 400-nm radiation propagating in an SF_6 gas at a pressure of 0.5 atm, the group-velocity mismatch in the absence of the waveguide dispersion component calculated with the use of the experimental data from [101] (the parameter ΔK_0 in the third column of Table 2) is approximately equal to 0.049 cm^{-1} in its absolute value. This estimate shows that group-delay effects may become the main factor limiting the minimum pulse duration for the schemes synthesizing subfemtosecond and attosecond pulses with the use of high-frequency Raman-active vibrations, such as Raman modes of molecular hydrogen, for example (see the data presented in Table 2 and Fig. 21b). Two to three Stokes and anti-Stokes sidebands due to such Raman vibrations would be sufficient, as shown in Ref. [16], to synthesize a subfemtosecond light pulse.

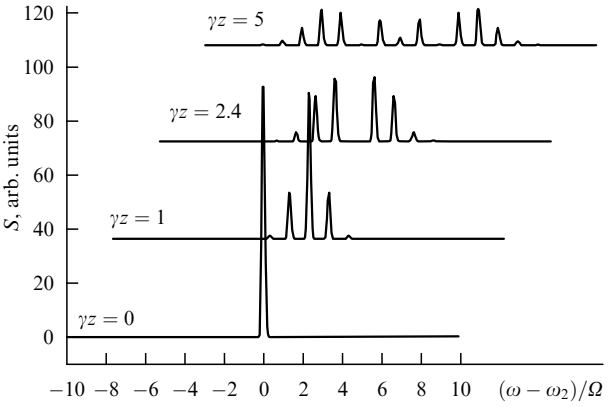

Figure 20. Spectral broadening of a probe pulse propagating in an impulsively pre-excited Raman-active medium. The pulse becomes dressed with equidistant Stokes and anti-Stokes sidebands with the frequencies $\omega_s = \omega_2 + s\Omega$ $(s = 0, \pm1, \pm2, \ldots)$, which are separated from each other by the frequency of molecular vibrations Ω.

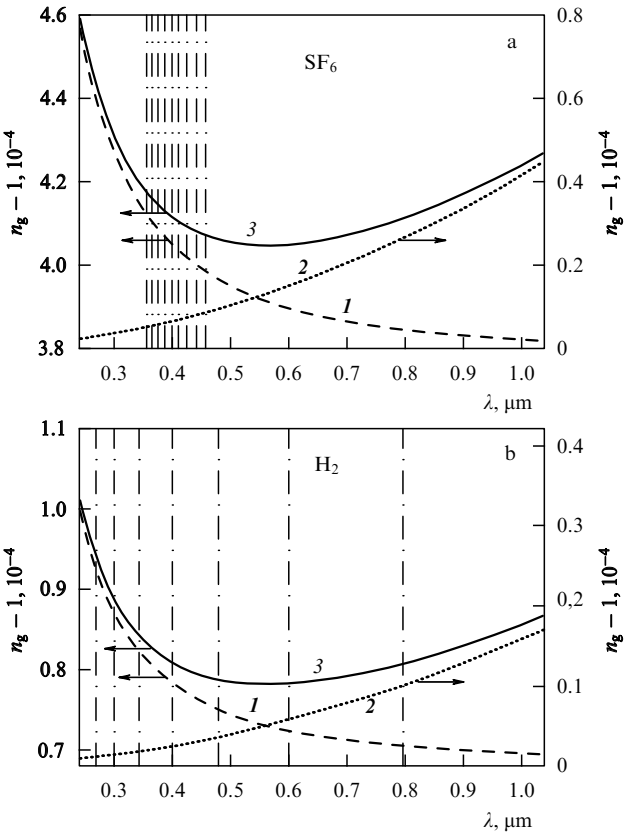

Figure 21. Group index $n_{\mathrm{g}} = c/v_{\mathrm{g}}$ as a function of the wavelength for (*1*) a gas without a fiber (based on the data from Ref. [101]), (*2*) the EH_{11} mode of an empty hollow fiber, and (*3*) the EH_{11} mode of a hollow fiber filled with a gas at a pressure of 0.5 atm in the case of (a) SF_6, $a = 42$ μm and (b) H_2, $a = 68$ μm (a is the inner radius of a hollow fiber). The vertical lines show the wavelengths of the probe pulse and Stokes and anti-Stokes components.

Table 2. Parameters of gases with intense Raman-active modes.

Gas	Δk, cm^{-1}	ΔK_0, cm^{-1}	a, μm	L_a	N
SF_6	775	0.049	42	30	22
N_2	2330	0.087	54	63	8
O_2	1555	0.07	49	45	11
CO_2	1388	0.094	40	25	12
H_2	4160	0.1	68	115	4

Notation: Δk is the frequency of Raman-active vibrations (from Ref. [101]); ΔK_0 is the group-velocity mismatch for pulses of 800- and 400-nm radiation in the gas in the absence of a hollow fiber calculated for a gas pressure of 0.5 atm with the use of the data from Ref. [101]; a is the optimal inner radius of a hollow fiber allowing group-velocity matching to be achieved for pulses of 800- and 400-nm radiation in the fundamental mode of the hollow fiber filled with a gas at a pressure of 0.5 atm; L_a is the attenuation length of 800-nm radiation in the fundamental mode of a hollow fiber with the optimal inner radius a corresponding to the group-velocity matching of 800- and 400-nm radiation pulses; and $N = [2c\Delta k\tau']^{-1}$ is the minimum number of Stokes and anti-Stokes components necessary to generate a pulse shorter than 1 fs ($\tau' = 1$ fs).

8.3 The ways to reduce the group-velocity mismatch in a hollow fiber

The group-velocity mismatch under the above-specified experimental conditions can be reduced by using the dispersion of waveguide modes. Physically, this opportunity is associated with the fact that the group velocity of a light pulse propagating in a gas-filled hollow fiber (solid lines in Fig. 21),

$$v^{pq} = \left(\frac{\partial K^{pq}}{\partial \omega}\right)^{-1}, \tag{72}$$

where K^{pq} is the propagation constant corresponding to the relevant waveguide mode of a hollow fiber with mode indices p and q, differs from the group velocity of a light pulse in the same gas, but in the absence of a waveguide (dashed lines in Fig. 21),

$$v = \left(\frac{\partial k}{\partial \omega}\right)^{-1} = \frac{c}{n}\left(1 + \frac{\omega}{n}\frac{\partial n}{\partial \omega}\right)^{-1}, \tag{73}$$

where $k = n\omega/c$ and n is the refractive index of the gas.

This difference in group velocities v^{pq} and v defined by Eqns (72) and (73) is due to the fact that the propagation constant of a light pulse in a gas-filled hollow fiber is related to the wave number k of this pulse in the same gas, but in the absence of the fiber by the expression $K^{pq} = (k^2 - h_{pq}^2)^{1/2}$, where the quantity h_{pq} can be found from the characteristic equation for the waveguide mode of a hollow fiber (the relevant wave-vector diagram is shown in Fig. 19).

In particular, using Eqn (30), we arrive at the following expression for the group velocity of a light pulse with a transverse field distribution corresponding to the EH_{1m} mode of a hollow fiber:

$$(v_l^m)^{-1} = (v_l)^{-1}\left[1 + \frac{1}{2}\left(\frac{u_l^m c}{a\omega_l n(\omega_l)}\right)^2\right], \tag{74}$$

where

$$v_l = \frac{c}{n(\omega_l)}\left[1 + \frac{\omega_l}{n(\omega_l)}\frac{\partial n}{\partial \omega}\bigg|_{\omega_l}\right]^{-1}$$

is the group velocity of the light pulse in the gas in the absence of a hollow fiber.

The group-velocity mismatch in a gas-filled hollow fiber can be then represented as a sum of two terms:

$$\Delta K_{mn} = \Delta K_0 + \Delta K_{mn}^{\mathrm{w}}, \tag{75}$$

where ΔK_0 and $\Delta K_{mn}^{\mathrm{w}}$ are the components of the group-velocity mismatch due to the gas and waveguide dispersion, respectively.

An important conclusion that follows from the fact that the group-velocity mismatch of short light pulses propagating in a gas-filled hollow fiber can be represented as a sum of group-velocity mismatch components related to the gas and waveguide dispersion is that the influence of group-delay effects on nonlinear-optical wave mixing in a hollow fiber can be reduced with an appropriate choice of the sort and the pressure of the gas filling the fiber, the inner radius of the fiber, and the waveguide modes involved in the nonlinear-optical process. The waveguide component of the group-velocity mismatch, as follows from Eqns (74) and (75), is inversely proportional to the square of the inner radius of a hollow fiber, scaling as

$$\Delta K_{mn}^{\mathrm{w}} \propto a^{-2}.$$

Physically, this circumstance implies that larger group-velocity mismatches can be compensated in hollow fibers with smaller inner diameters.

Dispersion curves for the group indices of Raman-active gases SF_6 and H_2 at a pressure of 0.5 atm are shown by the dashed lines in Fig. 21. The dotted lines in the same figures represent the dispersion curves for the group indices of the EH_{11} modes of hollow fibers with inner radii of 42 μm (Fig. 21a) and 68 μm (Fig. 21b). The resulting dispersion curves of the group indices including the waveguide dispersion are shown by the solid lines in these figures. With an appropriate choice of hollow-fiber parameters, as can be seen from the dependences presented in Fig. 21, the group-delay mismatch can be compensated within a sufficiently broad spectral range.

The third column of Table 2 presents the values of the group-velocity mismatch ΔK_0 for light pulses of 800- and 400-nm radiation in various gases with intense Raman-active modes (the frequencies of Raman-active vibrations Δk are presented in the second column of this table) at a gas pressure $p = 0.5$ atm. The walk-off length for pulses with such wavelengths in an SF_6 gas at a pressure of 0.4 atm, which was employed in experiments [14–16], is approximately 40 cm under these conditions. Group-delay effects may have a considerable influence on the generation of Stokes and anti-Stokes sidebands in such a situation, imposing limitations on the duration of light pulses synthesized in this way. The group-velocity mismatch can be completely compensated, on the other hand, for light pulses of 800- and 400-nm radiation by choosing the inner radius of a hollow fiber equal to 47 μm and using the fundamental waveguide mode to propagate each of these pulses.

The group-velocity mismatch of the pump and probe pulses can also be compensated in a similar way for other gases (see Table 2).

8.4 Generation of multiple Stokes and anti-Stokes sidebands and group-delay-free synthesis of ultrashort pulses

If the group-velocity mismatch ΔK_{mn} is small, Eqn (69) for the envelope of the probe pulse can be rewritten as

$$B(\tau, z) = B(\tau, 0) \sum_{s=-\infty}^{\infty} J_s(\gamma z) \exp(-\mathrm{i}s\Omega\tau), \qquad (76)$$

where $J_s(x)$ is the sth-order Bessel function. As can be seen from Eqn (76), multiple Stokes and anti-Stokes components arise in the spectrum of the probe pulse as this pulse propagates through an impulsively pre-excited Raman active gas and becomes dressed with Stokes and anti-Stokes sidebands. The number of these sidebands increases with the growth in the pump energy (leading to an increase in the parameter γ) and the interaction length (see Fig. 20) which is no longer limited by the walk-off length of the pump and probe pulses.

The minimum pulse duration that can be achieved by compensating the chirp of the pulse described by Eqn (76) is determined by the number M of Stokes and anti-Stokes components generated in the process of pulse propagation: $\tau \approx (2c\Delta kM)^{-1}$ (see also Table 2). Due to the properties of Bessel functions, the maximum value of M, in turn, is determined by the parameter γL (where L is the length of the Raman-active medium) in accordance with the approximate formula $M \approx \gamma L$. Thus, large interaction lengths are crucial for synthesizing ultrashort light pulses. The increase of the interaction length is, however, limited by group-delay effects (see Fig. 21) and group-velocity dispersion (Fig. 22).

Fortunately, with an appropriate choice of hollow-fiber parameters, the waveguide dispersion component, as can be seen from Figs 21 and 22, reduces the group delay and group-velocity dispersion for Stokes and anti-Stokes components within a broad spectral range. This circumstance is especially important for gases with high-frequency Raman-active vibrations. In the case of molecular hydrogen at a pressure of 0.5 atm, for example, the lengths corresponding to the group delay of Stokes components and a probe pulse with a wavelength of 400 nm equal to half the period of molecular vibrations are estimated in the absence of a hollow fiber as 37, 21, and 16 cm for the first, second, and third Stokes components, respectively. The use of a hollow fiber with an inner radius of 68 μm under these conditions (Figs 21b, 22b) would allow these characteristic walk-off lengths to be increased up to 57, 47, and 500 cm for the first, second, and third Stokes components, respectively.

Thus, the compensation of the group-velocity mismatch of the pump and probe pulses due to the use of the waveguide dispersion of a hollow fiber allows the efficiency of synthesizing ultrashort pulses through the generation of multiple Stokes and anti-Stokes sidebands in a Raman-active medium to be considerably improved. It should be mentioned here that the increase in the length of a hollow fiber inevitably leads to the growth in the magnitude of optical losses for leaky modes of a hollow fiber, which are always characterized by substantially nonzero attenuation coefficients (the characteristic attenuation lengths are summarized in the fifth column of Table 2). One promising way to solve this problem is to employ hollow-core fibers with a cladding having a structure of a two-dimensional photonic crystal — the so-called holey (or photonic-crystal) fibers [27–31]. The presence of a photonic band gap in the transmission spectrum of the cladding of such fibers permits optical losses characteristic of the leaky modes of hollow waveguides to be substantially reduced [32, 33] (see Section 9 of this review).

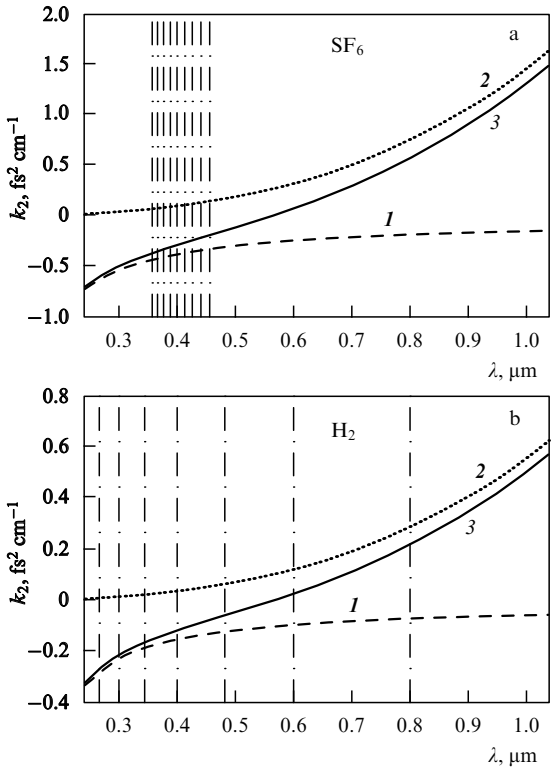

Figure 22. Group-velocity dispersion k_2 as a function of the wavelength for (*1*) a gas without a fiber (based on the data from Ref. [101]), (*2*) the EH_{11} mode of an empty hollow fiber, and (*3*) the EH_{11} mode of a hollow fiber filled with a gas in the case of (a) SF_6, $a = 42$ μm and (b) H_2, $a = 68$ μm. The gas pressure is 0.5 atm. The vertical lines show the wavelengths of the probe pulse and Stokes and anti-Stokes components.

The analysis performed above shows that the group-velocity mismatch of the pump and probe pulses may limit the minimum duration of ultrashort pulses produced through the generation of multiple Stokes and anti-Stokes sidebands in a Raman-active medium pre-excited with a short laser pulse. The use of hollow fibers in such experiments allows the efficiency of ultrashort-pulse synthesis to be considerably improved not only due to the increase in the length of nonlinear-optical interaction of light pulses in a Raman-active gas, but also due to the possibility of reducing the group-velocity mismatch of ultrashort pulses by using the waveguide dispersion of a hollow fiber. Having represented the group-velocity mismatch of short light pulses propagating through a gas-filled hollow fiber as a sum of components related to the gas dispersion and the dispersion of waveguide modes, we demonstrated that the influence of group-delay effects on stimulated Raman scattering in an impulsively excited gas can be considerably reduced with an appropriate choice of the sort and the pressure of the gas filling the fiber, the inner diameter of the hollow fiber, and waveguide modes involved in the impulsive excitation of the medium and the Raman-scattering process. The number of Stokes and anti-Stokes sidebands can be considerably increased under these conditions, which opens the way to decreasing the minimum duration of light pulses synthesized with the use of this approach.

8.5 Selective excitation of Raman-active modes

In this section, we will discuss a coherence-control technique that permits more Stokes and anti-Stokes sidebands to be generated without increasing the propagation length in a Raman-active gas, thus allowing shorter pulses to be synthesized and the influence of dispersion effects to be reduced. One of the simplest modifications of such a coherence-control approach is illustrated in Fig. 23. This method is based on the idea of replacing a single short pump pulse, which is usually employed to impulsively excite a Raman mode, by a sequence of N short light pulses.

The time interval T between the pulses in this sequence is chosen equal to a multiple of the period of the Raman-active mode $T_0 = 2\pi/\Omega$. The vibration amplitude of the Raman-active mode is then described by the following expression [102]:

$$Q(t) = Q_0(T)\sin(\Omega t + \varphi), \tag{77}$$

where

$$\varphi = \pi\frac{T}{T_0}(N-1), \tag{78}$$

$$Q_0(T) = \frac{C}{\Omega}\frac{\sin(\pi NT/T_0)}{\sin(\pi T/T_0)}, \tag{79}$$

and C is a constant.

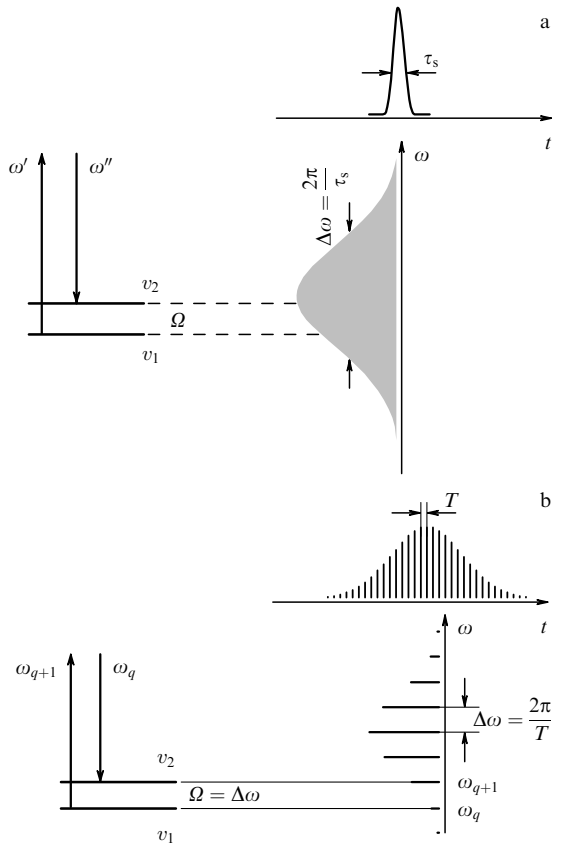

Figure 23. (a) Nonselective excitation of Raman-active modes with a single short pulse with a broad spectrum. (b) Resonant selective excitation of Raman-active modes with a sequence of short light pulses. Fourier transform of a periodic pulse sequence gives a comb of equidistant modes. The spectral separation $\Delta\omega = \omega_{q+1} - \omega_q$ between the neighboring modes in this comb is determined by the interpulse time interval T in the pulse train. Molecular vibrations are efficiently excited when the condition of a Raman resonance is satisfied, $\Delta\omega = 2\pi/T = \Omega/p$, where p is an integer.

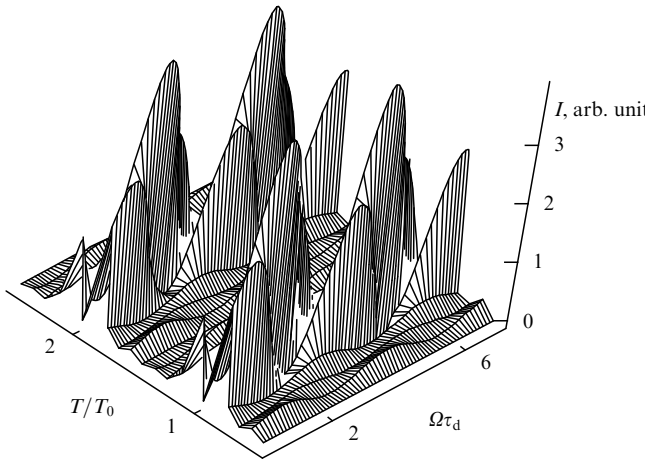

Figure 24. Intensity of the anti-Stokes signal, proportional to the amplitude of molecular vibrations squared, calculated as a function of $\Omega\tau_d$ (where τ_d is the delay time between the excitation and the probing of the medium) and the ratio T/T_0 for the case when the Raman mode is excited with a four-pulse sequence ($N = 4$).

Expressions (77)–(79) reveal resonances in the dependence of the amplitude of molecular vibrations on the interpulse separation in a periodic pulse sequence. The resonances in the dependence $Q(T)$ show up when the time interval T is equal to the period T_0 of the Raman-active mode (Fig. 24). Physically, these resonances are a result of the in-phase excitation of vibrations by a periodic external force whose period is a multiple of the period of molecular vibrations. In contrast to the case when a Raman-active mode is excited with a single short pulse, a resonant sequence of short pulses allows Raman vibrations to be excited in a selective way. To understand more aspects in the resonant behavior of the amplitude of molecular vibrations as a function of the interval between the pulses in a pulse sequence and to appreciate the consequences of this behavior for short-pulse synthesis in an impulsively excited Raman-active medium, it is very instructive to consider excitation of molecular vibrations in the frequency domain. The Fourier transform of a periodic pulse sequence gives a comb of equidistant modes. The separation $\Delta\omega$ between the neighboring modes in this comb is exactly tuned to a resonance with the frequency of the Raman mode (see Fig. 23): $\Delta\omega = 2\pi/T = \Omega/p$, where p is an integer. The resonant amplitude of molecular vibrations is proportional to the number of pulses in the train, which allows the efficiency of Raman excitation of a gas medium to be improved (see Fig. 24).

Table 3 provides a list of simple Raman-active molecules having short vibrational periods and high intensities of Raman lines, which seem to be promising for the synthesis of ultrashort pulses. To quantify the intensity of Raman scattering, we use the parameter introduced by Schrötter and Klöckner [103] (see also Ref. [104]).

Experimentally, resonant sequences of short pulses, allowing a selective excitation of Raman-active modes, can be produced with the use of spatial light modulators [105–111] which are capable of generating pulses with a virtually arbitrary temporal waveform. In particular, as demonstrated by experiments [25–27], periodic sequences of femtosecond pulses with appropriately chosen periods of pulses produced with the use of spatial light modulators can be employed to

Table 3. Parameters of Raman-active molecules with short periods of Raman vibrations and high intensities of Raman scattering.

Molecule	$\Omega/2\pi c$, cm^{-1}	Σ_j [103, 104]	T_0, fs
H_2	4156	3.7	8.0
HF	3962	1.0	8.4
H_2O	3652	3.4	9.1
NH_3	3334	6.3	10
C_6H_6	3070	14	11
C_2H_4	3019	6.6	11
CH_4	2914	8.6	11
HCl	2886	3.1	12
H_2S	2611	7.1	13
N_2	2331	1.0	14
N_2O	2224	0.4	15
CO	2143	0.9	16
NO	1877	0.4	18
O_2	1555	1.1	21
CO_2	1285	2.0	26

Notation: $\Omega/2\pi c$, Raman frequency; Σ_j, parameter introduced in Ref. [103] to characterize the intensity of Raman scattering relative to the Raman scattering intensity of the 2331-cm^{-1} mode in molecular nitrogen; T_0, vibrational period.

selectively prepare ground- or excited-state wave packets of potassium molecules [26, 27] and to steer multiphoton transitions in sodium atoms [25] in the gas phase. An important advantage of using spatial light modulators for the selective resonant excitation of Raman gases is associated with the fact that such modulators would provide an opportunity of automatic feedback optimization of frequency combs and pulse sequences with the use of optimal-control algorithms [28, 112–114].

9. Periodic-cladding hollow waveguides: the way to reduce optical losses

The waveguiding of radiation in conventional fibers is achieved due to total internal reflection. In the case of hollow fibers, the refractive index of the core is lower than the refractive index of the cladding. The propagation constants of waveguide modes in hollow fibers have, therefore, nonzero imaginary parts, and optical losses are inherent in the propagation of light in such fibers. This circumstance limits the fiber length in nonlinear-optical experiments, imposing restrictions on the enhancement of the nonlinear signal generated through harmonic generation and wave mixing. In this section, we will show that the use of hollow waveguides with a periodic cladding allows optical losses inherent in hollow-waveguide modes to be considerably reduced.

The idea of lowering the magnitude of optical losses in a hollow waveguide with a periodic cladding relative to the magnitude of optical losses in a hollow waveguide with a solid cladding is based on the high reflectivity of the periodic structure within the photonic band gap [115, 116]. To illustrate this idea, we will employ the geometric-optic approach to the analysis of radiation propagation in a waveguide.

Physically, attenuation of radiation propagating in a hollow waveguide is due to optical losses accompanying the reflection of radiation from waveguide walls. The attenuation coefficient α can then be found from the following relation [115]:

$$R^{2S} = \exp(-\alpha L), \tag{80}$$

where R is the reflection coefficient and S is the number of reflections from waveguide walls per length L. For a waveguiding layer (a fiber core) with a size a, the quantity S is given by

$$S = \frac{L}{2a\tan\theta}. \tag{81}$$

Here, θ is the angle of incidence, which can be expressed in terms of the propagation constant K and the transverse component of the wave number h as

$$h\tan\theta = K. \tag{82}$$

Using Eqns (80)–(82), we arrive at the following expression for the attenuation coefficient:

$$\alpha = -\frac{h}{aK}\ln R. \tag{83}$$

In the case of a hollow fiber, the reflection coefficient R is determined by standard Fresnel formulas. For TE waves making small angles θ with waveguide walls, we derive then [115]

$$\alpha_h^l = \frac{l^2\lambda^2}{n_1 a^3 (n_2^2 - n_1^2)^{1/2}}, \tag{84}$$

where n_1 and n_2 are the refractive indices of the waveguiding layer and the cladding, respectively, and l is an integer corresponding to the mode index.

Thus, the magnitude of optical losses in this case scales as λ^2/a^3, which is typical of hollow waveguides. This scaling law often prevents one from using long hollow waveguides in the case when a small core size is necessary to achieve a high power density of laser radiation.

This problem can be solved by using a hollow waveguide with a periodic cladding. Suppose that the refractive index of the waveguiding layer is equal, as before, to n_1, but the cladding now consists of alternating layers with refractive indices n_1 and n_2. Then, the coefficient of reflection from waveguide walls can be written as [115]

$$R_{\mathrm{PBG}} = -\mathrm{i}\varkappa^*\sinh(sNd)\left[s\cosh(sNd) + \mathrm{i}\,\frac{\Delta\beta}{2}\sinh(sNd)\right]^{-1}, \tag{85}$$

where

$$s^2 = \varkappa^*\varkappa - \left(\frac{\Delta\beta}{2}\right)^2, \tag{86}$$

$$\Delta\beta = 2\bar{n}\,\frac{\omega}{c}\cos\theta - \frac{2\pi m}{d} = 2\bar{n}\,\frac{\omega-\omega_0}{c}\cos\theta \tag{87}$$

is the detuning from the Bragg resonance for a periodic structure of the waveguide cladding with a period d; ω_0 is the central frequency of the photonic band gap of the cladding, $\bar{n} = \left[(n_1^2 + n_2^2)/2\right]^{1/2}$; m is an integer; d is the modulation period of the refractive index in the cladding; N is the number of periods in the waveguide cladding; and $\varkappa$ is the coefficient of coupling of forward and backward waves in the periodic cladding. In the case of a TE wave with $m = 1$, this coupling coefficient can be written as [115]

$$\varkappa = \frac{\sqrt{2}\,\mathrm{i}(n_2^2 - n_1^2)}{\lambda\cos\theta(n_2^2 + n_1^2)^{1/2}}. \tag{88}$$

Around the center of the photonic band gap, where $|\Delta\beta| \ll |\varkappa|$, we have [115]

$$R_{\mathrm{PBG}} = \tanh\left(|\varkappa| Nd\right). \tag{89}$$

For sufficiently large arguments of the hyperbolic tangent in Eqn (89), the lowering of the magnitude of optical losses in a hollow waveguide with a periodic cladding relative to a hollow waveguide with a solid cladding is characterized by the ratio

$$\frac{\alpha_{\mathrm{PBG}}}{\alpha_{\mathrm{h}}} \propto a \exp\left(-2|\varkappa| Nd\right). \tag{90}$$

As can be seen from Eqn (90), the increase in the number of periods in the cladding of a hollow waveguide leads to an exponential decrease in the magnitude of optical losses of waveguide modes relative to the magnitude of optical losses in a conventional hollow waveguide.

Thus, hollow waveguides with a periodic cladding allow optical losses characteristic of hollow-waveguide modes to be considerably reduced. As the number of periods of the cladding is increased, the magnitude of optical losses decreases exponentially. Therefore, hollow waveguides with a periodic cladding offer much promise for increasing the efficiency of nonlinear-optical interactions, including self- and cross-phase modulation, harmonic generation, and wave mixing.

Since hollow-core photonic-crystal fibers [117–126] belong to this class of waveguides, we anticipate that these fibers may be very useful for enhancing nonlinear-optical interactions. However, the structure of cladding in photonic-crystal fibers is, of course, much more complicated than the structure of a periodic multilayer considered above. Therefore, a more detailed analysis of waveguide modes and dispersion properties of photonic-crystal fibers is necessary to find optimal regimes of nonlinear-optical processes in such fibers.

10. Planar hollow corrugated photonic band-gap waveguides

10.1 A hollow waveguide with properties of a one-dimensional photonic crystal

One promising way of further enhancement of nonlinear-optical interactions and improvement of phase and group-velocity matching involves the creation of optical components integrating the properties of hollow waveguides and photonic band-gap structures. Photonic band-gap structures (or photonic crystals) are extensively employed nowadays for both fundamental research and the creation of practical optical components [127–129].

Numerous applications of such structures are based on their reflection, transmission, and dispersion properties, related to the existence of photonic band gaps in their transmission spectra and dispersion relations. One-dimensional PBG structures are employed as multilayer mirrors [130, 131], pulse compressors [132–134], narrow-band filters [115, 135], optical limiters and switches [136, 137], logic gates [138], and compact frequency converters [139–142]. More complicated, two-dimensional photonic crystals are used to create compact waveguides, decouplers, and multiplexers, as well as novel optical fibers. Such structures also serve for the engineering of new laser materials [143].

Below, we will consider the possibilities offered by a compact optical element consisting of a diffraction grating and a mirror (or another diffraction grating). The possibility of creating a one-dimensional PBG structure based on a grating pair has been previously discussed by Todori and Hayase [144]. The results of transmission measurements performed in Ref. [144] on a grating pair were interpreted with the use of a simple formula for a one-dimensional PBG structure neglecting waveguiding effects. We will show below that the waveguiding properties of a grating–mirror PBG structure play a very important role, having a noticeable influence on the transmission and dispersion of such a structure, considerably extending its filtering and phase-matching capabilities, and providing additional degrees of freedom in controlling the dispersion of guided modes.

10.2 Mode coupling and dispersion properties of a planar hollow PBG waveguide

To illustrate the main properties of a planar hollow waveguide consisting of a metal diffraction grating and a metal mirror (Fig. 25), we will employ a standard approach based on coupled-mode equations [55, 115]. Within the framework of this approach, the periodic modulation of the refractive index introduced by the grating is treated as a perturbation coupling forward and backward modes of an unperturbed waveguide. Around Bragg resonances, this coupling is especially strong, giving rise to photonic band gaps.

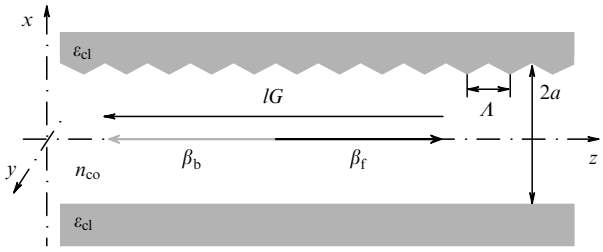

Figure 25. Mirror and diffraction grating combined to form a planar hollow corrugated waveguide: Λ is the period of the grating, $2a$ is the separation between the grating and the mirror, n_{co} is the refractive index of the waveguiding layer, and $\varepsilon_{\mathrm{cl}}$ is the dielectric constant of the cladding. The photonic band gap in the dispersion relation and transmission spectrum of such a structure arises due to a strong coupling of forward and backward waveguide modes with propagation constants β_{f} and β_{b} around the Bragg resonance (97).

The electric field inside a corrugated planar waveguide can be represented as a superposition of modes of an unperturbed planar waveguide (shown in Fig. 26) with unknown slowly varying envelopes [55, 115]:

$$\mathbf{E} = \frac{1}{2}\sum_n \mathbf{f}_n(x)\left[A_n(z)\exp\left(\mathrm{i}\beta_n z\right) + B_n(z)\exp\left(-\mathrm{i}\beta_n z\right)\right] \times \exp\left(-\mathrm{i}\omega t\right) + \mathrm{c.c.}, \tag{91}$$

where ω is the radiation frequency; β_n and $\mathbf{f}_n(x)$ are the propagation constant and the transverse field distribution for the nth mode of the planar waveguide, respectively; $A_n(z)$ and $B_n(z)$ are the slowly varying envelopes of the forward and backward waveguide modes with the mode index n.

Perturbation of the dielectric function $\Delta\varepsilon(x)$ due to the spatial modulation introduced by the grating gives rise to an

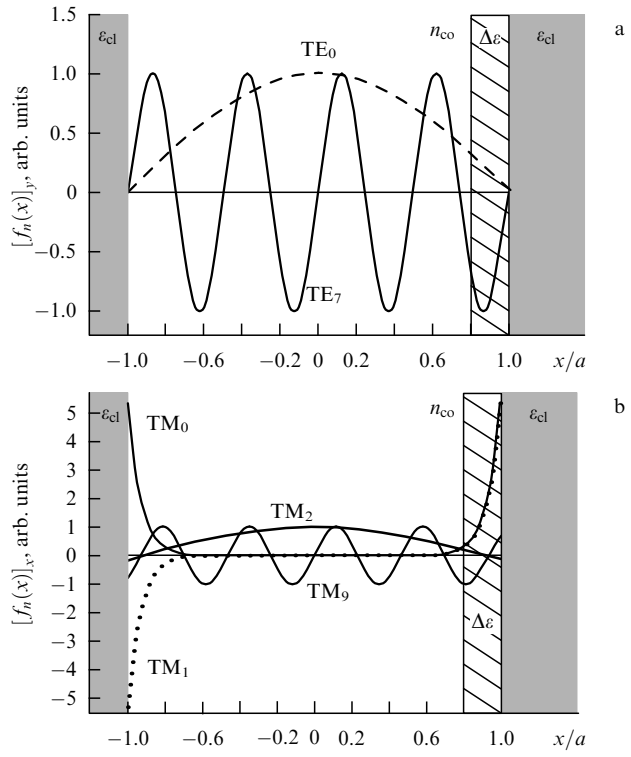

Figure 26. Electric-field distribution in guided modes of a planar hollow PBG waveguide: projections of the mode field amplitude (a) on the y-axis, $\left([f_n(x)]_y\right)$, for the TE$_0$ and TE$_7$ modes and (b) on the x-axis, $\left([f_n(x)]_x\right)$, for the TM$_0$, TM$_1$, TM$_2$, and TM$_9$ modes of a planar waveguide with aluminum-coated walls. The air-gap half-width is 11 μm, the refractive index of the waveguiding layer is 1, and the wavelength is 0.62 μm. The hatched areas show the region of nonzero perturbation of the dielectric function.

additive to the polarization equal to

$$\tilde{\mathbf{P}} = \Delta\varepsilon(x,z)\,\mathbf{E}\,. \tag{92}$$

Whenever $\Delta\varepsilon(x,z)$ is a scalar quantity, no coupling between TE and TM modes arises, and TE and TM modes are coupled in an independent way [55, 115]. Since the perturbation introduced by a diffraction grating in the case under study is periodic along the z-axis, this perturbation can be expanded as a Fourier series:

$$\Delta\varepsilon(x,z) = \sum_l \tilde{\varepsilon}_l(x)\exp(\mathrm{i}lGz)\,, \tag{93}$$

where $G = 2\pi/\Lambda$ is the reciprocal lattice constant and Λ is the period of the grating.

The set of equations for the envelopes of coupled modes is then written as [55, 115]

$$\frac{\mathrm{d}A_n}{\mathrm{d}z} = \sum_{m,l}\alpha_{nml}\left\{A_m\exp\left[\mathrm{i}(\beta_m-\beta_n+lG)z\right] + B_m\exp\left[-\mathrm{i}(\beta_m+\beta_n-lG)z\right]\right\}, \tag{94}$$

$$\frac{\mathrm{d}B_n}{\mathrm{d}z} = \sum_{m,l}\alpha_{nml}\left\{A_m\exp\left[\mathrm{i}(\beta_m+\beta_n-lG)z\right] + B_m\exp\left[-\mathrm{i}(\beta_m-\beta_n+lG)z\right]\right\}, \tag{95}$$

$$\alpha_{nml} = \frac{2\pi\mathrm{i}\omega^2}{\beta_n c^2}\,\frac{\int\tilde{\varepsilon}_l(x)\,\mathbf{f}_m(x)\,\mathbf{f}_n^*(x)\,\mathrm{d}x}{\int\left|\mathbf{f}_n(x)\right|^2\mathrm{d}x}\,. \tag{96}$$

With $\alpha_{\mathrm{fb}l} \neq 0$, a forward mode with a mode index 'f' and a backward mode with a mode index 'b' are especially strongly coupled when the Bragg resonance condition,

$$\beta_\mathrm{f} + \beta_\mathrm{b} = lG\,, \tag{97}$$

where l is an integer, is satisfied. In this regime, an efficient energy exchange between forward and backward modes occurs in a corrugated planar waveguide.

Figure 27 gives a general idea of how the photonic band gap is produced in a corrugated planar hollow waveguide. Many waveguide modes were simultaneously excited in PBG waveguides studied in our experiments, where structures with large air gaps between the grating and the mirror (the air-gap half-width $a = 10-44$ μm) were used. In such a situation, the broad photonic band gap observed in experiments is a result of overlapping of photonic band gaps corresponding to a family of strongly coupled modes meeting the Bragg-resonance condition of Eqn (97).

Figure 27 also shows the effective refractive index for the waveguide propagation regime, defined as $n_\mathrm{eff} = \tilde{\beta}_n/k$, where $\tilde{\beta}_n$ is the propagation constant of the nth mode in the corrugated planar waveguide. This effective refractive index provides an idea of the phase velocities of the coupled modes, allowing phase-matching abilities of the created PBG waveguide to be understood. The lower panel of Fig. 27 displays the experimentally measured (see Section 10.3) TM-mode transmission of a planar hollow PBG waveguide with the air-gap half-width a equal to 22 μm. The Bragg-resonance condition in the photonic band gap is met for two integers l and l' (G is the reciprocal-lattice vector).

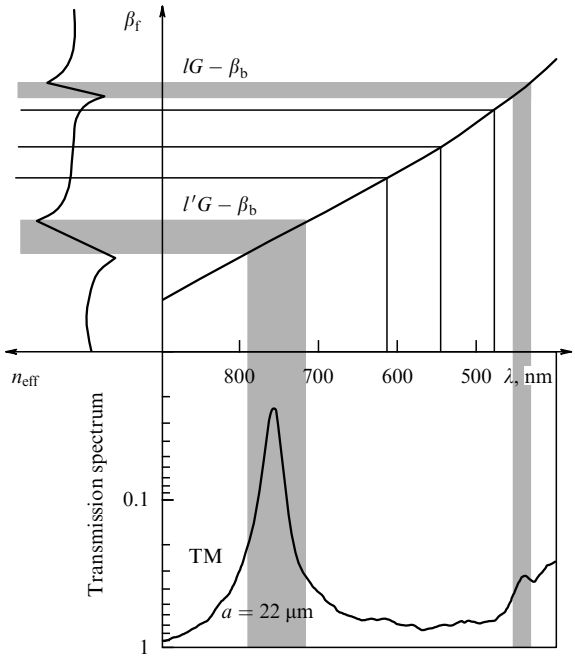

Figure 27. Dispersion relations, effective refractive index, and the photonic band gap for a planar hollow PBG waveguide: photonic band gaps corresponding to a family of strongly coupled modes meeting the Bragg-resonance condition (97) overlap to form a broad photonic band gap in transmission. The effective refractive index $n_\mathrm{eff} = \tilde{\beta}_n/k$, where $\tilde{\beta}_n$ is the propagation constant of the nth guided mode in the corrugated planar waveguide, provides an idea of the phase velocities of the coupled modes and allows phase-matching abilities of the PBG waveguide to be analyzed.

10.3 Transmission spectra and enhancement of nonlinear-optical processes

The element implementing the idea of a compact optical component combining the properties of a hollow waveguide and a PBG structure consists of an aluminum-coated diffraction grating and an aluminum-coated mirror [145]. Our experiments were performed with 1200- and 2400-grooves mm^{-1} diffraction gratings, which allowed the photonic band gaps to be observed in the visible range. The waveguiding length of the structure was equal to 6 cm. The separation between the grating and the mirror was varied from 20 up to 100 μm. By changing this parameter, we were able to tune the photonic band gap in the transmission spectra of such structures (Fig. 28).

Transmission spectra of created planar hollow waveguides, as is seen from Fig. 28, feature photonic band gaps, whose positions and parameters are sensitive to the polarization of probing radiation and characteristics of the waveguide. As one might expect from Eqn (97), the photonic band gap for TM-polarized light is blue-shifted as the width of the waveguiding layer decreases (see Fig. 28). A decrease in the air gap between the grating and the mirror also leads to an increase in the magnitude and the width of the photonic band gap, which is due to the growth in the degree of light localization within the area of the perturbed dielectric function near the walls of the waveguide (see Fig. 26), resulting in a stronger coupling of forward and backward modes.

The results of experimental studies [145, 146] show that the above-described planar hollow PBG waveguide displays properties similar to the properties of planar corrugated waveguides. However, in contrast to a conventional corrugated dielectric waveguide, the light is guided in a gas (or whatever fills the gap between the grating and the mirror) in our structure, which permits such structures to be employed to guide high-intensity laser pulses, thus allowing many remarkable opportunities of gas-filled hollow waveguides demonstrated in the past few years by ultrashort-pulse generation, nonlinear-optical frequency conversion, and spectroscopic experiments to be considerably expanded.

Periodic perturbation of the refractive index introduced by the grating, giving rise to photonic band gaps, provides additional degrees of freedom in tuning the dispersion of the structure, opening new ways of phase and group-velocity matching of light pulses and appealing for soliton research. We anticipate that the efficiency of nonlinear-optical processes can be improved in such waveguides due to the local-field enhancement, which is characteristic of PBG structures [146, 147]. Finally, localization of light near a metal-coated grating surface in lowest order TM modes in the waveguide (see Fig. 26) allows effects related to the photonic band-gap structure to be effectively enhanced.

Planar hollow PBG waveguides permit dispersion tailoring within the frequency range accessible to many widespread lasers, including lasers generating short pulses. Such structures may be, therefore, very useful for many practical applications, including pulse compression, high-order harmonic generation, and nonlinear-optical gas-phase analysis. In particular, self-phase modulation, which is employed for pulse compression, and multiwave mixing processes can be substantially enhanced in such waveguides due to local-field effects.

The efficiency of frequency conversion through high-order harmonic generation and wave mixing can be improved due to phase and group-velocity matching. With an appropriate choice of a resonant gas and the width of the gap between the grating and the mirror, such waveguide structures can be also used as optical filters whose transmission spectra may be tuned in a very practical way by simply changing the gas pressure.

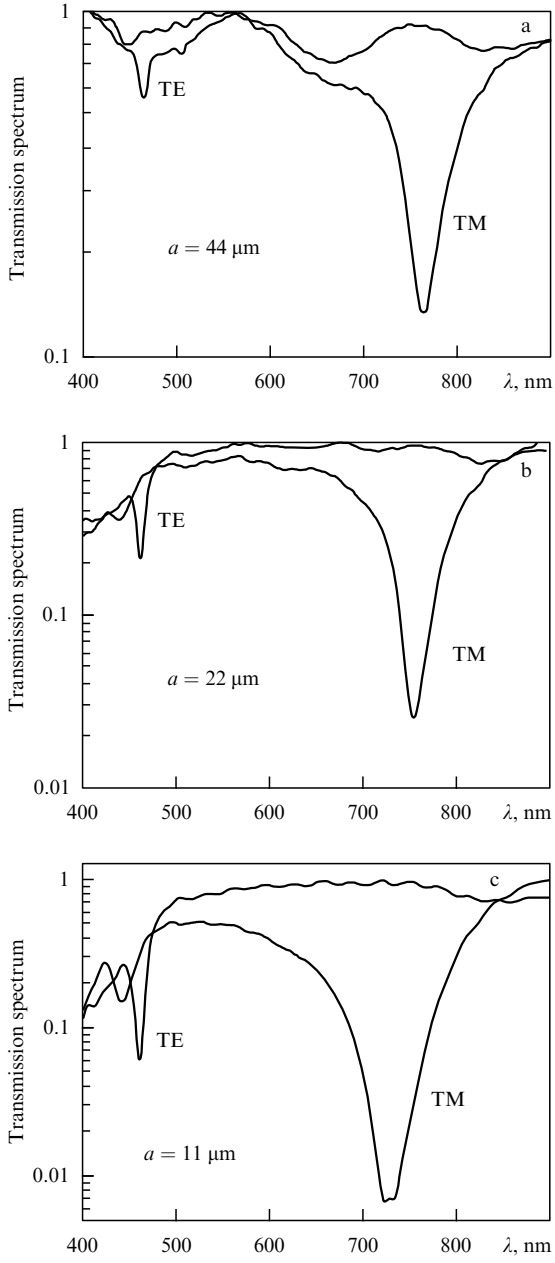

Figure 28. Transmission spectra of a planar corrugated hollow waveguide consisting of a 2400-grooves mm^{-1} aluminum-coated grating and an aluminum mirror (see Fig. 26) with an air-gap half-width a equal to 44 μm (a), 22 μm (b), and 11 μm (c).

11. Conclusions

The rapid conceptual and technological progress achieved in the optics of ultrashort pulses within the past five to seven years has had a significant impact on various areas of modern science. As a part of this process, ultrashort laser pulses evolved from a unique subject of research accessible only to

a few laboratories into a routine tool of laser experiments extensively employed in physics, chemistry, biology, biomedicine, and laser technologies. The examples of applications of gas-filled waveguides given above illustrate that such waveguides are an important element in the vast toolkit of ultrafast optics, which serves to successfully and efficiently solve several fundamental problems of nonlinear optics and ultrafast science.

The main physical processes underlying the successful use of hollow fibers for the efficient generation of unprecedentedly short light pulses, enhancement of coherent short-wavelength radiation generation, and improvement of the sensitivity of nonlinear-optical gas-phase analysis include self- and cross-phase modulation, coherent four-wave mixing, high-order harmonic generation, and stimulated Raman scattering. Self-phase modulation in hollow fibers allows a few-optical-cycle pulses with energies up to several tens of microjoules to be produced.

Stimulated Raman scattering has already been demonstrated to permit the generation of sub-4-fs pulses, and it opens the way to synthesize subfemtosecond pulses. Increased interaction lengths and improved phase and group-velocity matching attainable for ultrashort pulses in hollow fibers substantially enhance harmonic-generation and wave-mixing processes. These properties of hollow fibers offer much promise for the creation of sources capable of efficiently generating coherent short-wavelength radiation and for the improvement of the sensitivity of optical gas-phase analysis.

Harmonic generation and wave mixing combined with cross-phase modulation make it possible to produce extremely short pulses with simultaneous frequency conversion. New horizons for applying hollow waveguides in ultrafast optics are associated with the use of coherence-control methods for an optimal preparation of a medium for the maximum efficiency of harmonic generation and stimulated Raman scattering, as well as with the creation of new optical components integrating hollow waveguides with photonic band-gap structures.

Acknowledgments

I am deeply and sincerely grateful to A N Naumov, R B Miles, D von der Linde, V P Silin, F Giammanco, A B Fedotov, D A Sidorov-Biryukov, S De Silvestri, M Motzkus, J Haus, M Nisoli, S A Uryupin, A P Tarasevitch, and A M Sergeev for fruitful collaboration and illuminating discussions. I am thankful also to O N Krokhin for his useful comments on this review.

This study was supported in part by the President of Russian Federation Grant No. 00-15-99304, the Russian Foundation for Basic Research Grant No. 00-02-17567, CRDF Awards Nos. RP2-2266 and RP2-2275, and the Volkswagen Foundation project No. I/76 869.

References

1. Szipöcs R et al. *Opt. Lett.* **19** 201 (1994); Stingl A et al. *Opt. Lett.* **20** 602 (1995); Xu L et al. *Opt. Lett.* **21** 1259 (1996); Sutter D H et al. *Opt. Lett.* **24** 631 (1999)
2. Kopf D et al. *Opt. Lett.* **22** 621 (1997); Mayer E J et al. *Opt. Lett.* **22** 528 (1997); Kärtner F X et al. *Opt. Lett.* **22** 831 (1997)
3. Sartania S et al. *Opt. Lett.* **22** 1562 (1997); Xu L et al. *Appl. Phys. B* **65** 151 (1997); Poppe A et al. *IEEE J. Sel. Top. Quantum Electron.* **4** 179 (1998)
4. Brabec T, Krausz F *Rev. Mod. Phys.* **72** 545 (2000)
5. Pshenichnikov M S, Baltuska A, Wiersma D A, in *Conf. on Lasers and Electro-Optics-Europe*: *Intern. Quantum Electronics Conf.* (*CLEO/EUROPE-IQEC 2000*), *Nice, France, Sept. 10–15, 2000*, Conf. Digest, p. CMB7
6. Cerullo G et al., in *Proc. Second Italian-Russian Symp. on Ultrafast Optical Physics* (*ITARUS'99*), *Moscow, Feb. 22–25, 1999*: *Tribute to N.I. Koroteev* (Eds G Ferrante, M Vaselli, A M Zheltikov) (Moscow: Intellect Center, 2000) p. 141
7. Spielmann Ch et al. *Science* **278** 661 (1997)
8. Nisoli M, De Silvestri S, Svelto O *Appl. Phys. Lett.* **68** 2793 (1996)
9. Nisoli M et al. *Opt. Lett.* **22** 522 (1997)
10. Baltuska A et al. *Opt. Lett.* **22** 102 (1997)
11. Zhavoronkov N, Korn K, in *Conf. on Lasers and Electro-Optics* (*CLEO'2001*), *Baltimore, MD, USA, May 6–11, 2001*, Postdeadline Papers (Baltimore: OSA, 2001) p. CPD19-1
12. Paul P M et al. *Science* **292** 1689 (2001); Hentschel M et al. *Nature* **414** 509 (2001)
13. Nazarkin A, Korn G *Phys. Rev. A* **58** R61 (1998)
14. Korn G, Dühr O, Nazarkin A *Phys. Rev. Lett.* **81** 1215 (1998)
15. Nazarkin A et al. *Phys. Rev. Lett.* **83** 2560 (1999)
16. Wittmann M, Nazarkin A, Korn G *Phys. Rev. Lett.* **84** 5508 (2000)
17. Scrinzi A, Geissler M, Brabec T *Laser Phys.* **11** 169 (2001)
18. Milosevic N et al., in *10th Annual Intern. Laser Physics Workshop* (*LPHYS'01*), *Moscow, Russia, July 3–7, 2001*, Book of Abstracts, p. 73; Papadogiannis N A et al. *Phys. Rev. Lett.* **83** 4289 (1999); Tempea G et al. *Phys. Rev. Lett.* **87** 109401 (2001)
19. Reichert J et al. *Phys. Rev. Lett.* **84** 3232 (2000)
20. Diddams S A et al. *Phys. Rev. Lett.* **84** 5102 (2000); Jones D J et al. *Science* **288** 635 (2000)
21. Holzwarth R et al. *Phys. Rev. Lett.* **85** 2264 (2000)
22. Zheltikov A M *J. Raman Spectrosc.* **31** 653 (2000); Zheltikov A M, in *Handbook of Vibrational Spectroscopy* Vol. 1 (Eds J Chalmers, P R Griffiths) (New York: Wiley, 2001) p. 572
23. Zewail A H (Ed.) *Femtochemistry*: *Ultrafast Dynamics of the Chemical Bond* (World Scientific Series in 20th Century Chemistry, Vol. 3) (Singapore: World Scientific, 1994); "Femtosecond Coherent Raman Spectroscopy". Special Issue (Ed. W Keifer) *J. Raman Spectrosc.* **31** (1/2) (2000)
24. Pausch R et al. *J. Raman Spectrosc.* **31** 7 (2000); Vierheilig A et al. *Chem. Phys. Lett.* **312** 349 (1999); Chen T et al. *Chem. Phys. Lett.* **325** 176 (2000)
25. Hornung T et al. *Appl. Phys. B* **71** 277 (2000)
26. Hornung T, Meier R, Motzkus M *Chem. Phys. Lett.* **326** 445 (2000)
27. Hornung T et al. *Chem. Phys.* **267** 261 (2001)
28. Zeidler D et al. *Phys. Rev. A* **64** 023420 (2001)
29. Shen Y R *The Principles of Nonlinear Optics* (New York: J. Wiley, 1984)
30. Reintjes J F *Nonlinear Optical Parametric Processes in Liquids and Gases* (New York: Academic Press, 1984)
31. Balcou P et al. *J. Phys. B*: *At. Mol. Opt.* **25** 4467 (1992)
32. Macklin J J, Kmetec J D, Gordon III C L *Phys. Rev. Lett.* **70** 766 (1993)
33. Bellini M et al. *Phys. Rev. Lett.* **81** 297 (1998); Zerne R et al. *Phys. Rev. Lett.* **79** 1006 (1997); Ditmire T et al. *Phys. Rev. Lett.* **77** 4756 (1996)
34. Chang Z et al. *Phys. Rev. Lett.* **79** 2967 (1997)
35. Villoresi P et al. *Phys. Rev. Lett.* **85** 2494 (2000); Altucci C et al. *J. Opt. A*: *Pure Appl. Opt.* **2** 289 (2000)
36. von der Linde D et al. *Phys. Rev. A* **52** R25 (1995); Tarasevitch A et al. *Phys. Rev. A* **62** 023816 (2000)
37. Zheltikov A M, Thesis for Doctorate of Physicomathematical Sciences (Moscow: Physics Department, Moscow State Univ., 1999); Zheltikov A M *Vestn. Mosk. Univ. Ser. Fiz. Astron.* **42** (4) 3 (2001)
38. Miles R B, Laufer G, Bjorklund G C *Appl. Phys. Lett.* **30** 417 (1977)
39. Arkhipkin V G et al. *Kvantovaya Elektron.* (Moscow) **12** 1420 (1985) [*Sov. J. Quantum Electron.* **15** 938 (1985)]
40. Durfee III C G et al. *Opt. Lett.* **22** 1565 (1997)
41. Koroteev N I, Zheltikov A M *Appl. Phys. B* **67** 53 (1998)
42. Zheltikov A M, Koroteev N I, Naumov A N *Zh. Eksp. Teor. Fiz.* **115** 1561 (1999) [*JETP* **88** 857 (1999)]
43. Rundquist A et al. *Science* **280** 1412 (1998)
44. Tamaki Y, Midorikawa K, Obara M *Appl. Phys. B* **67** 59 (1998)

45. Constant E et al. *Phys. Rev. Lett.* **82** 1668 (1999)
46. Durfee III C G et al. *Phys. Rev. Lett.* **83** 2187 (1999)
47. Fedotov A B et al. *Appl. Phys B* **72** 575 (2001); *Laser Phys.* **11** 515 (2001)
48. Naumov A N et al. *Pis'ma Zh. Eksp. Teor. Fiz.* **73** 300 (2001) [*JETP Lett.* **73** 263 (2001)]; *Zh. Eksp. Teor. Fiz.* **120** 280 (2001) [*JETP* **93** 247 (2001)]
49. Zheltikov A M, Naumov A N *Kvantovaya Elektron.* (Moscow) **30** 351 (2000) [*Quantum Electron.* **30** 351 (2000)]; Naumov A N, Giammanco F, Zheltikov A M *Laser Phys.* **10** 774 (2000)
50. Durfee III C G et al. *Opt. Lett.* **24** 697 (1999)
51. Akhmanov S A, Nikitin S Yu *Fizicheskaya Optika* (Physical Optics) (Moscow: Izd. MGU, 1998)
52. Naumov A N, Zheltikov A M *Laser Phys.* **11** 424 (2001)
53. Kolevatova O A, Naumov A N, Zheltikov A M *Kvantovaya Elektron.* (Moscow) **31** 173 (2001) [*Quantum Electron.* **31** 173 (2001)]; Kolevatova O A, Naumov A N, Zheltikov A M *Laser Phys.* **11** 427 (2001)
54. Marcatili E A J, Schmeltzer R A *Bell Syst. Tech. J.* **43** 1783 (1964)
55. Adams M J *An Introduction to Optical Waveguides* (Chichester: Wiley, 1981)
56. Akhmanov S A, Vysloukh V A, Chirkin A S *Optics of Femtosecond Laser Pulses* (New York: AIP, 1992)
57. Backus S et al. *Opt. Lett.* **21** 665 (1996)
58. Fedotov A B et al. *Opt. Commun.* **133** 587 (1997)
59. Tempea G, Brabec T *Opt. Lett.* **23** 762 (1998); Milosevic N, Tempea G, Brabec T *Opt. Lett.* **25** 672 (2000)
60. Naumov A N et al. *J. Opt. Soc. Am. B* **18** 811 (2001)
61. Naumov A N et al. *Laser Part. Beams* **19** 75 (2001)
62. Alfano R R et al. *Opt. Lett.* **11** 626 (1986)
63. Alfano R R et al. *Phys. Rev. A* **35** 459 (1987); Alfano R R et al. *Appl. Opt.* **26** 3491 (1987)
64. Agrawal G P *Nonlinear Fiber Optics* (Boston: Academic Press, 1989)
65. Ho P P et al. *J. Opt. Soc. Am. B* **7** 276 (1990)
66. Dianov E M et al. *Kvantovaya Elektron.* (Moscow) **15** 1941 (1988) [*Sov. J. Quantum Electron.* **18** 1211 (1988)]
67. Agrawal G P, Baldeck P L, Alfano R R *Phys. Rev. A* **40** 5063 (1989)
68. Gladkov S M et al. *Pis'ma Zh. Tekh. Fiz.* **14** 1399 (1988) [*Sov. Tech. Phys. Lett.* **14** 610 (1988)]
69. Fedotov A B et al. *J. Opt. Soc. Am. B* **8** 363 (1991)
70. Zheltikov A M, Koroteev N I, Fedotov A B *Opt. Spektrosk.* **72** 971 (1992) [*Opt. Spectrosc.* **72** 527 (1992)]
71. Zheltikov A M, Koroteev N I, Fedotov A B *Laser Phys.* **4** 569 (1994); Fedotov A B, Koroteev N I, Zheltikov A M *Laser Phys.* **5** 835 (1995)
72. Fedotov A B et al. *Phys. Lett. A* **271** 407 (2000)
73. Siders C W et al. *J. Opt. Soc. Am. B* **13** 330 (1996)
74. Fedotov A B et al. *J. Nonlinear Opt. Phys. Mater.* **6** 387 (1997)
75. Chang Z et al. *Phys. Rev. A* **58** R30 (1998)
76. Salières P, L'Huillier A, Lewenstein M *Phys. Rev. Lett.* **74** 3776 (1995)
77. Zuo T et al. *Phys. Rev. A* **51** 3991 (1995)
78. Figueira de Morisson Faria C, Milošević D B, Paulus G G *Phys. Rev. A* **61** 063415 (2000); Milošević D B, Becker W, Kopold R *Phys. Rev. A* **61** 063403 (2000); Milošević D B, Becker W *Phys. Rev. A* **62** R011403 (2000)
79. Watson J B et al. *Phys. Rev. A* **53** R1962 (1996); Sanpera A et al. *Phys. Rev. A* **54** 4320 (1996)
80. Sekikawa T et al. *Phys. Rev. Lett.* **83** 2564 (1999)
81. Silin V P *Zh. Eksp. Teor. Fiz.* **47** 2254 (1964) [*Sov. Phys. JETP* **20** 1510 (1965)]; **114** 864 (1998) [*JETP* **87** 468 (1998)]; *Kvantovaya Elektron.* (Moscow) **26** 11 (1999) [*Quantum Electron.* **29** 11 (1999)]; *Zh. Eksp. Teor. Fiz.* **117** 926 (2000) [*JETP* **90** 805 (2000)]; Akhmanov S A et al., Preprint of Physics Department of Moscow State University, No. 5 (Moscow: Moscow State Univ., 1988)
82. Schafer K J et al. *Phys. Rev. Lett.* **70** 1599 (1993)
83. Corkum P B *Phys. Rev. Lett.* **71** 1994 (1993)
84. Lewenstein M et al. *Phys. Rev. A* **49** 2117 (1994)
85. Lewenstein M, Salières P, L'Huillier A *Phys. Rev. A* **52** 4747 (1995)
86. Antoine Ph et al. *Phys. Rev. A* **53** 1725 (1996)
87. Zheltikov A M et al. *Laser Phys.* **6** 49 (1996)
88. Antoine Ph, L'Huillier A, Lewenstein M *Phys. Rev. Lett.* **77** 1234 (1996)
89. Antoine Ph et al. *Phys. Rev. A* **56** 4960 (1997)
90. Naumov A N et al. *Laser Phys.* **11** 286 (2001)
91. Ammosov M V, Delone N B, Kraĭnov V P *Zh. Eksp. Teor. Fiz.* **91** 2008 (1986) [*Sov. Phys. JETP* **64** 1191 (1986)]
92. Harris S E, Sokolov A V *Phys. Rev. Lett.* **81** 2894 (1998)
93. Sokolov A V, Yavuz D D, Harris S E *Opt. Lett.* **24** 557 (1999)
94. Sokolov A V et al. *Phys. Rev. Lett.* **85** 562 (2000); Fam Le Kien et al. *Phys. Rev. A* **60** 1562 (1999)
95. Corkum P B, Burnett N H, Ivanov M Y *Opt. Lett.* **19** 1870 (1994)
96. Ivanov M et al. *Phys. Rev. Lett.* **74** 2933 (1995)
97. von der Linde D *Appl. Phys. B* **68** 315 (1999)
98. Farkas G, Toth C *Phys. Lett. A* **168** 447 (1992)
99. Harris S E, Macklin J J, Hänsch T W *Opt. Commun.* **100** 487 (1993)
100. Christov I P, Murnane M M, Kapteyn H C *Phys. Rev. Lett.* **78** 1251 (1997)
101. Carman R L, Mack M E *Phys. Rev. A* **5** 341 (1972)
102. Akhmanov S A, Nikitin S Yu *Physical Optics* (Oxford: Clarendon Press, 1997)
103. Schrötter H W, Klöckner W, in *Raman Spectroscopy of Gases and Liquids* (Topics in Current Physics, Vol. 11, Ed. A Weber) (Berlin: Springer-Verlag, 1979) p. 123
104. Akhmanov S A, Koroteev N I *Metody Nelineĭnoĭ Optiki v Spektroskopii Rasseyaniya Sveta* (Methods of Nonlinear Optics in Light Scattering Spectroscopy) (Moscow: Nauka, 1981)
105. Weiner A M et al. *Opt. Lett.* **15** 326 (1990)
106. Hillegas C W et al. *Opt. Lett.* **19** 737 (1994)
107. Weiner A M *Prog. Quantum Electron.* **19** 161 (1995)
108. Weiner A M et al. *IEEE J. Quantum Electron.* **28** 908 (1992)
109. Wefers M M, Nelson K A *Opt. Lett.* **18** 2032 (1993)
110. Wefers M M, Nelson K A *Science* **262** 1381 (1993)
111. Wefers M M, Nelson K A *J. Opt. Soc. Am. B* **12** 1343 (1995)
112. Brumer P, Shapiro M *Chem. Phys. Lett.* **126** 54 (1986)
113. Tannor D J, Kosloff R, Rice S A *J. Chem. Phys.* **85** 5805 (1986)
114. Judson R S, Rabitz H *Phys. Rev. Lett.* **68** 1500 (1992)
115. Yariv A, Yeh P *Optical Waves in Crystals* (New York: Wiley, 1984)
116. Zheltikov A M *Laser Phys.* **11** 435 (2001)
117. Knight J C et al. *Opt. Lett.* **21** 1547 (1996)
118. Birks T A, Knight J C, Russell P St J *Opt. Lett.* **22** 961 (1997)
119. Knight J C et al. *Science* **282** 1476 (1998)
120. Cregan R F et al. *Science* **285** 1537 (1999); Knight J C et al. *Opt. Mater.* **11** 143 (1999)
121. Broderick N G R et al. *Opt. Lett.* **24** 1395 (1999); Monro T M et al. *Opt. Lett.* **25** 206 (2000)
122. Fedotov A B et al. *Pis'ma Zh. Eksp. Teor. Fiz.* **71** 407 (2000) [*JETP Lett.* **71** 281 (2000)]
123. Ranka J K, Windeler R S, Stentz A J *Opt. Lett.* **25** 25 (2000)
124. Zheltikov A M *Usp. Fiz. Nauk* **170** 1203 (2000) [*Phys. Usp.* **43** 1125 (2000)]; in *Nanoscale Linear and Nonlinear Optics: Intern. School on Quantum Electronics, Erice, Sicily, July 2–14, 2000* (AIP Conf. Proc., Vol. 560, Eds M Bertolotti, C M Bowden, C Sibilia) (Melville, N.Y.: AIP, 2001) p. 259; in *Proc. of the Third Intern. Symp. on Modern Problems of Laser Physics* (*MPLP'2000*), *Novosibirsk, Russia, 2000* (Eds S N Bagayev, V I Denisov) (Novosibirsk: Inst. Laser Phys., 2000) p. 11
125. Fedotov A B et al. *Laser Phys.* **10** 723 (2000); Alfimov M V et al. *Pis'ma Zh. Eksp. Teor. Fiz.* **71** 714 (2000) [*JETP Lett.* **71** 489 (2000)]; Fedotov A B et al. *Laser Phys.* **11** 138 (2001)
126. Zheltikov A M et al. *Zh. Eksp. Teor. Fiz.* **120** 570 (2001) [*JETP* **93** 499 (2001)]; Fedotov A B et al. *Appl. Phys. B* **72** 575 (2001)
127. Yablonovitch E *J. Opt. Soc. Am. B* **10** 283 (1993)
128. *Photonic Band Gap Materials* (NATO ASI Series. Ser. E, Vol. 315, Ed. C M Soukoulis) (Dordrecht: Kluwer Acad. Publ., 1996)
129. Joannopoulos J D, Meade R D, Winn J N *Photonic Crystals* (Princeton, N.J.: Princeton Univ. Press, 1995)
130. Born M, Wolf E *Principles of Optics* (Oxford: Pergamon Press, 1980)
131. Yokoyama H et al. *Appl. Phys. Lett.* **57** 2814 (1990); Baba T et al. *IEEE J. Quantum Electron.* **27** 1347 (1991); Jung I D et al. *Appl. Phys. B* **65** 137 (1997)
132. Cerullo G et al. *Opt. Lett.* **24** 1529 (1999)
133. Dühr O et al. *Opt. Lett.* **24** 34 (1999)
134. Koroteev N I et al. *Opt. Commun.* **159** 191 (1999)
135. Wang S S, Magnusson R *Appl. Opt.* **34** 2414 (1995)

136. Scalora M et al. *Phys. Rev. Lett.* **73** 1368 (1994)
137. Tran P *Opt. Lett.* **21** 1138 (1996); *J. Opt. Soc. Am. B* **16** 70 (1999); Scholz S, Hess O G, Ruhle R *Opt. Express* **3** 28 (1998)
138. Kashkarov P K, Zheltikov A M *Nonlinear Opt.* **23** 305 (2000); Nefedov I S et al. *Laser Phys.* **10** 640 (2000)
139. Martorell J, Vilaseca R, Corbalán R *Appl. Phys. Lett.* **70** 702 (1997)
140. Scalora M et al. *Phys. Rev. A* **56** 3166 (1997); Centini M et al. *Phys. Rev. E* **60** 4891 (1999)
141. Tarasishin A V, Zheltikov A M, Magnitskiĭ S A *Pis'ma Zh. Eksp. Teor. Fiz.* **70** 800 (1999) [*JETP Lett.* **70** 819 (1999)]; Zheltikov A M, Tarasishin A V, Magnitskiĭ S A *Zh. Eksp. Teor. Fiz.* **118** 340 (2000) [*JETP* **91** 298 (2000)]
142. Dumeige Y et al. *Appl. Phys. Lett.* **78** 3021 (2001)
143. *Nanoscale Linear and Nonlinear Optics*: *Intern. School on Quantum Electronics, Erice, Sicily, July 2 – 14, 2000* (AIP Conf. Proc., Vol. 560, Eds M Bertolotti, C M Bowden, C Sibilia) (Melville, N.Y.: AIP, 2001)
144. Todori K, Hayase S *Appl. Phys. Lett.* **70** 550 (1997)
145. Fedotov A B et al. *Laser Phys.* **11** 1009 (2001)
146. Fedotov A B et al. *J. Opt. Soc. Am. B* **19** 1162 (2002)
147. Zheltikov A M, in *CLEO/Europe – EQEC Focus Meetings, Munich, Germany, June 18 – 21, 2001*, Conf. Digest (Munich: EPS, 2001) p. 248